# 3 Silo and hopper design for strength

J. MICHAEL ROTTER

## 3.1 Introduction

Silos and hoppers are widely used in a great many different industries for storing a huge range of different solids. The sizes of these silos may vary from capacities less that 1 tonne to the largest containing as much as 100 000 tonnes. The size of the silo has a strong bearing on the number of different considerations required: small silos generally do not produce structural problems, but in large silos many different aspects need careful attention.

The designs used for silos also vary very much (Figure 3.1). In some industries (e.g. grain storage), there is a competitive industry producing standard silo products which function extremely well and cost-effectively provided the conditions remain those anticipated. In other industries (e.g. cement and mineral ore storage) very large silos are used and every silo must be individually designed for the special conditions. It should be noted that each silo is normally designed to contain a very limited range of solids, and that the use of a silo designed for one kind of solid to store different solids can easily cause damage. Bulk solids vary very much in their properties, and a silo that is perfectly adequate to store one material may be very dangerous for another.

The terms *silo*, *bunker*, *bin* and *hopper* are often used to refer to similar containers in different industries. Here, the word 'hopper' is exclusively used with a special meaning for the converging part leading to a gravity discharge outlet. All complete storage containers are referred to as silos, irrespective of the stored solid, geometry and industrial sector. A characteristic form to describe the parts of the silo is shown in Figure 3.2. The transition, which lies at the junction between the vertical wall and the hopper, should be noted.

This chapter provides a brief outline of the development of understanding of pressures that develop in silos and their consequences for the safety of the silo structure. More structural failures occur in silos than in any other engineered structural form, considering the numbers of each, and these failures occur in all countries and all industries. Structural design considerations for silos are therefore a key aspect of bulk solids handling systems.

The chapter refers extensively to the provisions of the recently developed European standards for silo pressures (EN 1991-4 2007) and for metal silo structural design (EN 1993-4-1 2007), for which the author was the chief contributor and editor. Further useful information relating to the structural design of all silos may be found in Rotter (2001a).

## 3.2 Why pressures in silos matter

### 3.2.1 *General*

The pressures that develop in a silo are very different from those developing in a tank that contains fluid. Fluid pressures depend uniquely on the head, and in most fluid storages flow velocities are so low that dynamic effects are small. By contrast, pressures in silos

*Bulk Solids Handling: Equipment Selection and Operation* Edited by Don McGlinchey

 ISBN: 978-1-405-15825-1

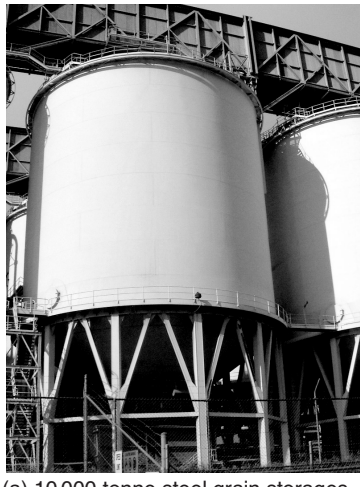

(a) 10 000 tonne steel grain storages, Australia

(b) Corrugated steel storage, Germany


(c) Rectangular concrete silo battery, Austria

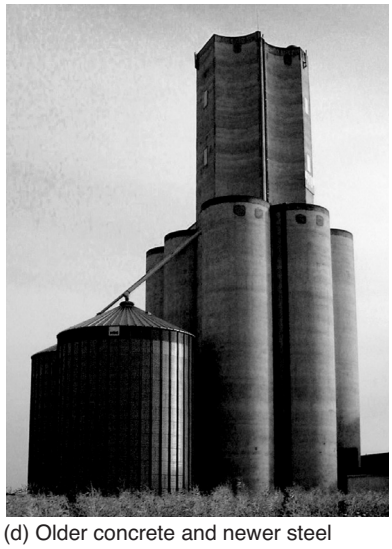

(d) Older concrete and newer steel silos, France

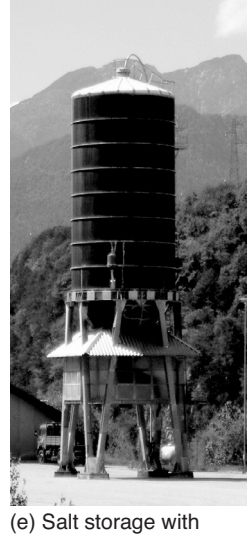

(e) Salt storage with control room, Italy

(f) FRP farm silo, France

**Figure 3.1** Different geometries and sizes of silo.

are dominated by frictional phenomena, the flow of bulk solids is controlled by frictional considerations and is largely independent of head, and there are few analogies between fluid and solid storage that are either valid or practically useful. In this context, it is worth noting that sound mechanics equations to describe fluid flow have existed for over a hundred years, but no comparable agreed set of equations yet exists to deal with bulk solids flow.

Pressures that develop in stored solids can have an important impact on their free flow from a silo if the bulk solid is prone to developing a small cohesive strength under stress

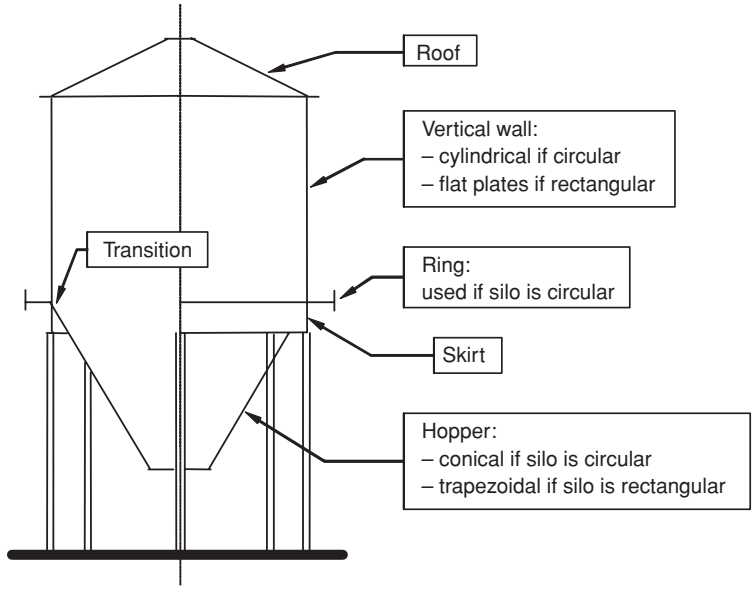


**Figure 3.2** Terminology for parts of a typical silo.

(e.g. flour). These aspects are dealt with in the accompanying chapter by Dr John Carson and are not commented on further here.

The most critical aspect of pressures in silos is their effect on the structure designed to contain the solid. Because the properties of solids vary widely, the pressures can also vary very much both in magnitude, distribution and stability. Some conditions lead to very unpredictable pressure peaks that can cause serious damage, whilst other arrangements are very benign and do not cause any concern even to the unwary. This chapter tries to make some clear distinctions between these different situations.

In particular, where pressures in silos are being defined for the purposes of structural design, an understanding of the consequences for the structure is absolutely vital. Thus, it is often imagined that high pressures, wherever and whenever occurring, are the most damaging event. This is very far from the truth, and many theories of silo pressure and scientific articles on pressures are very misleading because their authors did not understand what stress conditions would be induced in the structure by the pressures, nor the conditions that lead to structural failure. This chapter sets out some pointers to that information and it is hoped that the reader will appreciate that this subject is not straightforward, but a full explanation is beyond the scope of this chapter.

### 3.2.2 *Classifications of silos*

Silos are commonly classified according to the cross-sectional shape in plan section. Most silos are circular, but some are rectangular and interstitial gaps between adjacent circular silos may even be star-shaped. The pressure regime is principally important in silos of larger dimensions, and the circular silo dominates these: for this reason, this chapter is chiefly concerned with the circular planform.

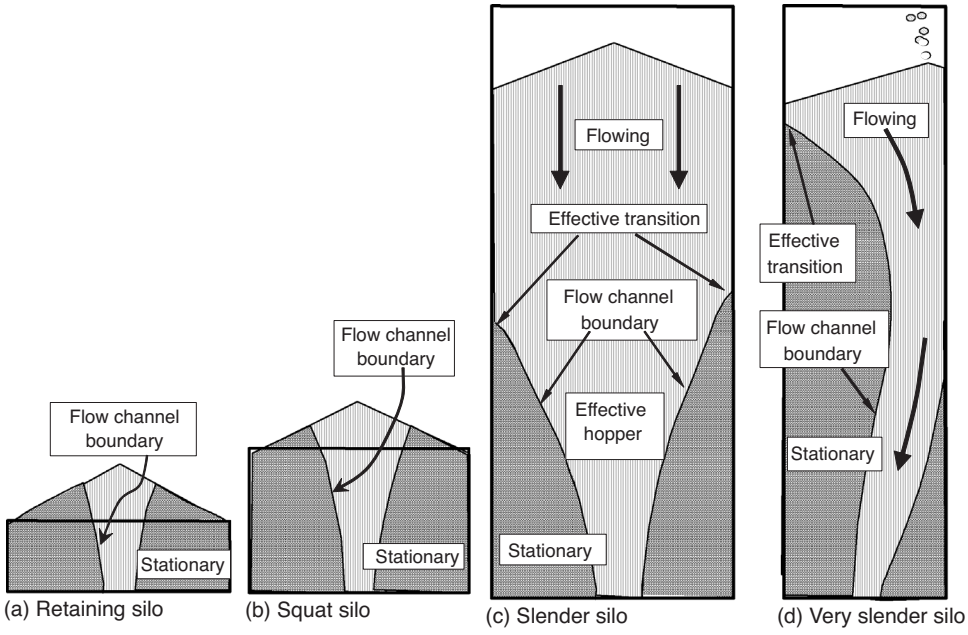


**Figure 3.3** Silo conditions for different aspect ratios.

A second key distinction is the overall size of the silo. Small silos do not present structural challenges and can be designed using fairly simple calculations. Very large silos need great attention to many details. For this reason, EN 1991-4 divides silos into three categories according to the mass of solid stored, and has different design requirements for each. The break points occur at 100 tonnes, 1000 tonnes (for special cases) and 10 000 tonnes. The standard on structural design of steel silos makes similar divisions, though at different values because it is concerned with aspects of the structure, not the loading. The break points occur at 100, 200 (with eccentric discharge), 1000 (elevated) and 5000 (ground supported) tonnes, with considerable design calculation effort being demanded where the largest sizes are used.

A third key classification is necessary to define the pressure regime. This is the aspect ratio (height $H$ divided by horizontal dimension $D$). Most silos research has studied slender silos ($H/D > 2$) and most of this chapter is concerned with this geometry. In squat silos ($H/D < 1$), the top surface profile plays an important role and issues of the difference between filling and discharge pressures are much reduced (Pieper & Stamou 1981). EN 1991-4 gives different rules for each aspect ratio, classing them as slender, intermediate, squat and retaining (Figure 3.3).

### 3.2.3 *Metal and concrete silos*

Metal and concrete silos carry their loads in very different ways, so the kinds of damage that can occur in each type are very different and the critical design considerations are different. For this reason, the later part of the chapter examines these two cases in separate sections.

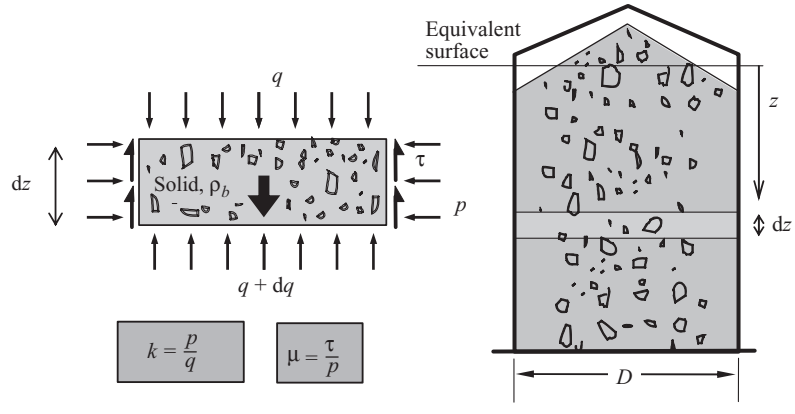


**Figure 3.4** Silo contents, notation and a slice of solid.

## 3.3 Pressures in silos: basic theory

### 3.3.1 *Early studies*

A brief historical account of the developing understanding of silos may seem strange in a chapter that advises on silo design and management, but there are good reasons for it. The field of silo pressures is full of misunderstandings and misinterpretations, and many of these continue and are repeated today, so an appreciation of the reasons for some misconceptions provides a valuable background.

Although silos have been used to store solids (e.g. grains) for thousands of years, the earliest scientific studies of the pressures in silos were only undertaken at the end of the nineteenth century. Several researchers performed simple experiments and developed simple theories in this period (for a good description, see Ketchum 1907), but the most important of these was Janssen (1895) who both performed experiments on a tall square model silo and developed the theory which is almost universally used as the single reliable reference point in a sea of uncertainties concerning silo pressures.

### 3.3.2 *Janssen silo pressure theory for vertical walls*

This theory is so critical to understanding many aspects of silos that the derivation is set out here.

A tall silo with vertical walls, whose horizontal cross section can effectively take any shape, is shown in Figure 3.4. The equilibrium of forces on a slice of the solid with unit weight (or less formally bulk density) $\rho_b$ at some depth $z$ is shown, where the slice has height d$z$, plan area $A$ and perimeter against the wall $U$. The stresses acting on it may vary across the horizontal surface above and below, and around the perimeter with the wall, so the mean values are used in this analysis. The mean vertical stress is $q$, the consequential mean horizontal pressure against the wall $p$ and the frictional shear stress (termed frictional traction) on the wall $\tau$. Vertical equilibrium of this slice of solid leads to

$$(q + \mathrm{d}q)A + U\tau\,\mathrm{d}z = qA + \rho_b A\,\mathrm{d}z$$

or

$$\frac{\mathrm{d}q}{\mathrm{d}z}A + U\,\tau = \rho_{\mathrm{b}}A \tag{3.1}$$

The vertical stress $q$ on the slice need not be uniform: the analysis considers only the mean value. Horizontal equilibrium of the slice requires some symmetry to exist in the wall pressures $p$, but they need not be constant around the perimeter (this becomes a serious issue later). Shear stresses on the top and bottom of the slice are assumed to integrate to a zero resultant on each face.

Two assumptions are next made (as used by Janssen):

**a** The full wall friction is assumed to be developed against the wall at every point, so that the mean frictional shear $\tau$ is related to the mean normal pressure $p$ on the wall through the wall friction coefficient $\mu$ (Figure 3.4) as

$$\tau = \mu p \tag{3.2}$$

**b** The normal pressure $p$ (mean value around the perimeter) is deemed to be related to the mean vertical stress $q$ through a lateral pressure ratio $K$ (Figure 3.4) as

$$p = Kq \tag{3.3}$$

Inserting these into Equation (3.1) leads to

$$\frac{\mathrm{d}q}{\mathrm{d}z} + \frac{U}{A}\mu K q = \rho_{\mathrm{b}} \tag{3.4}$$

which may be solved to yield

$$q = q|_{z=0} = 0 + \frac{\rho_{\mathrm{b}}A}{\mu U}\left(1 - e^{-zU/(AK\mu)}\right) \tag{3.5}$$

If the *mean* vertical stress in the solid $q$ is taken as zero at some reference height $z = 0$ (Figure 3.4) (this condition is met at the centroid of the top pile of solids), then

$$q|_{z=0} = 0 \tag{3.6}$$

and Equation (3.5) can be more neatly written as

$$q = q_0(1 - e^{-z/z_0}) \tag{3.7}$$

in which

$$q_0 = \rho_{\mathrm{b}}\, z_0 \tag{3.8}$$

and

$$z_0 = \frac{1}{\mu K}\,\frac{A}{U} \tag{3.9}$$

Here, $q_0$ represents the mean vertical stress in the solid that is reached asymptotically at great depth. The length measure $z_0$ defines the rate at which the asymptote is approached and is commonly termed the *Janssen reference depth*.

The origin of the vertical coordinate $z$ (at the centroid of the top pile of solids) is called the *equivalent surface*.

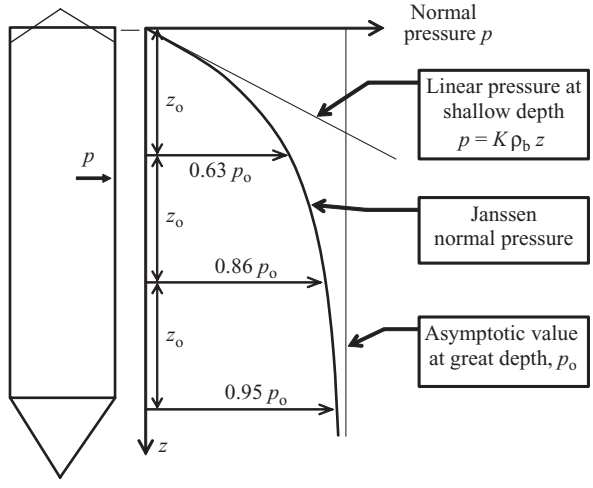


**Figure 3.5** Janssen pressure pattern.

It is natural to transform Equation (3.7) into pressures normal to the wall $p$ (Figure 3.4)

$$p = p_0(1 - e^{-z/z_0}) \tag{3.10}$$

in which the *asymptotic normal pressure* at great depth is given by

$$p_0 = \frac{\rho_b A}{\mu U} = K\rho_b z_0 \tag{3.11}$$

The typical pattern of pressure defined by this equation is shown in Figure 3.5.

Since many silos have circular cross sections, it is useful to simplify the above equations to specialise them for a silo of radius $R$.

$$z_0 = \frac{R}{2\mu K} \quad \text{and} \quad p_0 = \frac{\rho_b R}{2\mu} \tag{3.12}$$

The values of the wall friction coefficient $\mu$ and the lateral pressure ratio $K$ may be measured in control tests on the particular solid being stored (see Chapter 1).

A few deductions may be made from these equations. At great depth, the mean pressure $p$ depends only on the radius $R$ and the wall friction coefficient $\mu$, not on the depth below the surface. A smooth wall leads to higher pressures than a rough wall. The pressures all vary linearly with the solid bulk density $\rho_b$, so this is a key parameter in any silo evaluation.

The asymptotic value of pressure $p_0$ is actually more robust than the pressure distribution according to Janssen, because it does not need the assumption of a lateral pressure ratio. At great depth, conditions are stable, and neither the mean vertical stress $q$ nor the mean wall pressure $p$ changes. The equilibrium of a simple slice then simply equates the weight of the slice to the support given by wall friction, which becomes (adopting $\tau = \mu p$),

$$\mu p_0 U = \rho_b A \tag{3.13}$$

or

$$p_0 = \frac{\rho_b A}{\mu U} = \frac{\rho_b R}{2\mu} \tag{3.14}$$

Thus, every theory that assumes that the wall friction is fully developed must reach the same asymptotic value of lateral pressure $p_0$ at great depth. This applies whether the silo is just filled or is being emptied.

At shallow depths, the pressures vary linearly with depth and are approximated by

$$p = K\rho_b z \tag{3.15}$$

which is the 'earth pressure' against a retaining wall. However, this theory does not take proper account of the surface profile in defining wall pressures near the surface, and this matters in squat silo geometries (see EN 1991-4 2007).

The Janssen theory is the main descriptor of filling pressures in all standards.

### 3.3.3 *The lateral pressure ratio K*

The theory of Janssen was rapidly found to give quite a good representation of the pressures in a silo after it was filled. It is relatively easy to measure the bulk density $\rho_b$ and wall friction coefficient $\mu$, but the lateral pressure ratio $K$ was less easy. Both bulk granular solids and soils (which are granular solids) were not well understood in the early twentieth century, so it was natural that the earth pressure theory of Rankine (1857), which defined two limiting values of $K$, should be adopted as applicable in a silo. These are limiting values because, at these values, the solid is ready to deform by shearing into a different shape. They are the Rankine active and passive limits, given by

$$\text{Active} \quad K_a = \frac{1 - \sin\phi_i}{1 + \sin\phi_i} \tag{3.16}$$

$$\text{Passive} \quad K_p = \frac{1 + \sin\phi_i}{1 - \sin\phi_i} \tag{3.17}$$

where $\phi_i$ is the angle of internal friction of the solid, found by shearing the solid under a compressive stress normal to the plane of shearing. For a typical solid with $\phi_i = 30^\circ$, $K_a = 0.33$ and $K_p = 3.0$. The ratio of these two values is later found to be relevant and can be seen as $K_p/K_a = 9$.

In the first use of Janssen's theory (Koenen 1895), it was assumed that the solid in a silo after filling was in a Rankine active state, giving a low value of lateral pressure ratio $K$, and leading to smaller pressures. However, after extensive damage to many silos, it was widely recognised by the 1960s that this was an underestimate of $K$.

This situation is best explained using understandings that came much later. In Figure 3.6, a silo wall is retaining bulk solid. The pressure against the wall depends on the extent to which the wall moves inwards or outwards. In the limit, the two Rankine states are reached where the solid can deform plastically, but if the wall is rigid and does not move at all, a state referred to as $K_0$ exists. This is not far from the Rankine active state, but the value of $K_0$ is perhaps 50% larger than $K_a$. If the wall is flexible, the value of $K$ may fall slightly as it moves outwards. The stored bulk solid is essentially in an elastic state, not at a plastic limit.

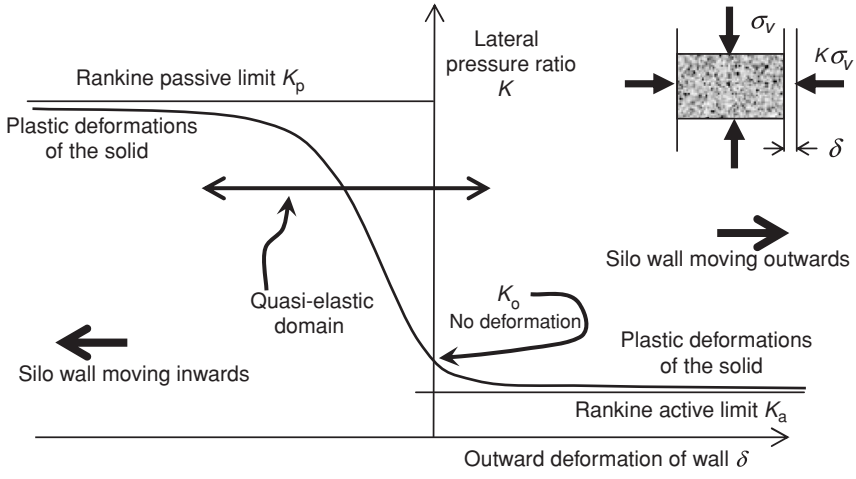


**Figure 3.6** Effect of wall horizontal movement on lateral pressure ratio $K$.

The value for $K_0$ has long been approximately related to the angle of internal friction $\phi_i$ of the solid (Jaky 1948) as

$$K_0 = 1 - \sin\phi_i \tag{3.18}$$

The background to this equation may be read in Muir Wood (1990).

The ideal $K_0$ relates to conditions in which the vertical and horizontal stresses are principal stresses and both uniform. Since the state of the silo after filling has both a non-uniform vertical stress pattern and shear stresses against the wall, it is best here to assign the value $K_f$ for the filling state, noting that $K_f > K_a$, but $K_f \approx > K_0$.

It is best to measure the lateral pressure ratio $K$ directly (see Chapter 1), but it has long been common to estimate it from the measured angle of internal friction $\phi_i$. Accounting for the above effects, the European standard EN 1991-4 (2007) defines the filling value of $K_f$ for design purposes as

$$K_f = 1.1(1 - \sin\phi_i) \tag{3.19}$$

### 3.3.4 *Pressures in hoppers*

The Janssen theory describes pressures in a parallel-sided vessel. The corresponding theory for a converging channel came much later, and is normally attributed to Walker (1964, 1966), though it was first derived by Dabrowski (1957) and was probably also found by Jenike and others in the late 1950s.

The hopper height is $H$ and the vertical coordinate is taken with its origin at the hopper apex, using coordinate $x$ (Figure 3.7). The steepest line on the hopper is at angle $\beta$ to the vertical. For a conical or pyramidal hopper, the horizontal coordinate to the closest point on the wall is $r = x \tan\beta$ and the area of a slice becomes

$$A = k_1 r^2 = k_1 x^2 \tan^2\beta \tag{3.20}$$

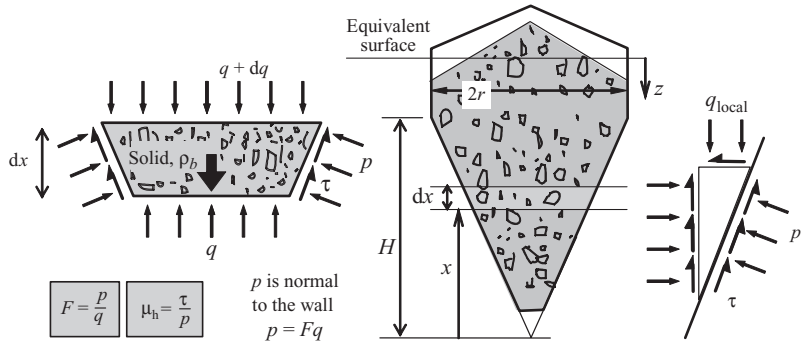


**Figure 3.7** Hopper slice analysis, coordinate system and local equilibrium.

where $k_1 = \pi$ for a conical hopper and $k_1 = 4$ for a square hopper of half side $r$. The perimeter of the slice is given by

$$U = k_2 r = k_2 x \ \tan\beta \tag{3.21}$$

where $k_2 = 2\pi$ for a conical hopper and $k_2 = 8$ for a square hopper of half side $r$. Vertical equilibrium of the slice of solid (Figure 3.7) leads to

$$\begin{aligned}&(q + dq)k_1(x + dx)^2 \ \tan^2\beta - qk_1x^2 \ \tan^2\beta + \rho_b\, k_1x^2 \ \tan^2\beta \mathrm{d}x \\ &\quad = (p \ \sin\beta + \tau \ \cos\beta)k_2x \ \tan\beta \frac{\mathrm{d}x}{\cos\beta}\end{aligned} \tag{3.22}$$

Cancelling, eliminating small terms and noting that $(k_2/k_1) = 2$ for both geometries

$$x\frac{\mathrm{d}q}{\mathrm{d}x} = 2\left(p + \frac{\tau}{\tan\beta} - q\right) - \rho_b x \tag{3.23}$$

in which $p$ is the mean normal pressure against the hopper wall, $q$ is the mean vertical stress in the solid, $\tau$ is the mean wall frictional traction and $\rho_b$ the bulk density.

The two assumptions used in the Janssen analysis are next made:

**a** The frictional shear $\tau$ is assumed to be a fixed proportion of the local normal pressure $p$. This is the hopper wall friction coefficient $\mu_h$ when sliding occurs, but is some smaller value, an effective friction $\mu_{h,\mathrm{eff}}$ when there is no sliding

$$\tau = \mu_h p \tag{3.24}$$

**b** The mean pressure normal on the inclined wall $p$ is deemed to be related to the mean vertical stress $q$ (Figure 3.7) through the hopper pressure ratio $F$ as

$$p = Fq \tag{3.25}$$

Inserting these into Equation (3.23) leads to

$$x\frac{\mathrm{d}q}{\mathrm{d}x} - 2q[F + F\mu_h \ \cot\beta - 1] = -\rho_b x \tag{3.26}$$

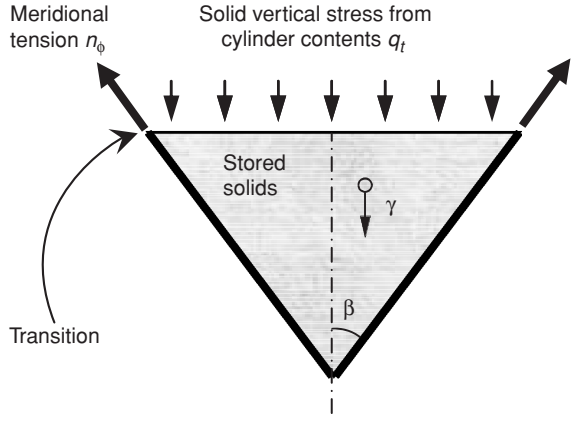


**Figure 3.8** Mean vertical stress at the transition and overall hopper equilibrium.

or

$$x\frac{\mathrm{d}q}{\mathrm{d}x} - n\,q = -\rho_{\mathrm{b}} x \tag{3.27}$$

in which

$$n = 2[F + F\mu_{\mathrm{h}}\cot\beta - 1] \tag{3.28}$$

which may be solved, considering the top boundary condition $q = q_{\mathrm{t}}$ at $x = H$, to yield

$$q = q_{\mathrm{t}}\left(\frac{x}{H}\right)^n + \frac{\rho_{\mathrm{b}} H}{(n-1)}\left\{\left(\frac{x}{H}\right) - \left(\frac{x}{H}\right)^n\right\} \tag{3.29}$$

where $q_{\mathrm{t}}$ is the mean vertical stress in the solid at the transition (Figure 3.8).

It is evident that the value of $F$ must depend on geometry and solids properties, just as $K$ was dependent on solids properties in the analysis of the pressures on vertical walls.

The normal pressures may be deduced from Equation (3.29) as

$$p = F\left[q_{\mathrm{t}}\left(\frac{x}{H}\right)^n + \frac{\rho_{\mathrm{b}} H}{(n-1)}\left\{\left(\frac{x}{H}\right) - \left(\frac{x}{H}\right)^n\right\}\right] \tag{3.30}$$

Equation (3.30) gives a variety of different forms for the hopper pressure distribution, depending on the value of $F$. The two components of loading are clearly separated: the weight of solids in the hopper (term involving $\rho_{\mathrm{b}} H$) and the pressure derived from the cylinder (transition surcharge $q_{\mathrm{t}}$). Equation (3.30) indicates that high local pressures can occur at the transition if the barrel has a moderate height and $F$ is high. The distribution becomes very peaked at the transition for high $n$ which arises if $F$ is high and the hopper is steep and rough. This theory is used in EN 1991-4 (2007), but older standards (e.g. DIN 1055-6 1987) often gave empirical approximations to the pressure pattern which could not be guaranteed to be safe in all conditions.

These pressure patterns are illustrated in Figure 3.9, where the changing shape of the hopper wall pressures caused by transition vertical pressures $q_{\mathrm{t}}$ is illustrated for different values of $F$.

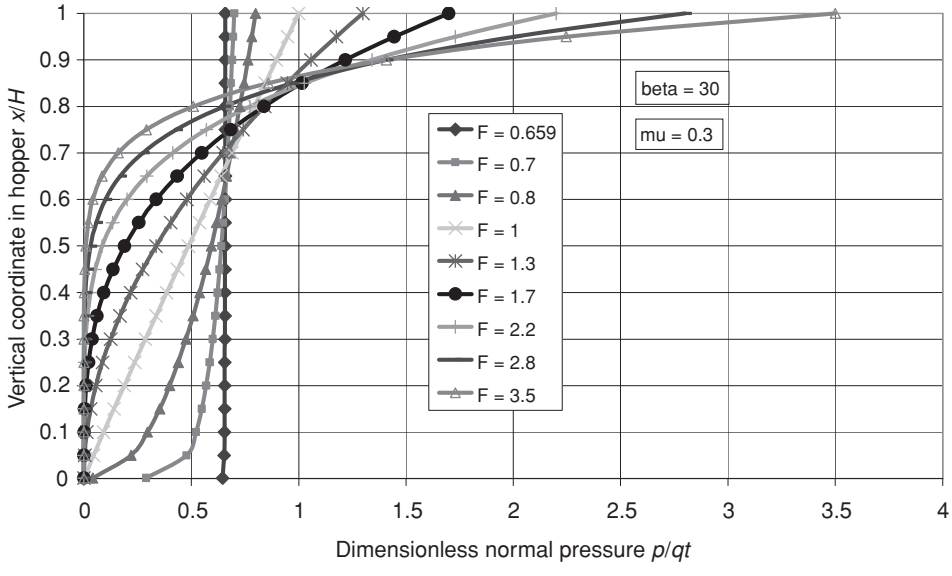


**Figure 3.9** Changing pattern of pressures in hoppers as the value of $F$ changes.

The question of whether the friction is fully mobilised in a hopper depends on its slope and the smoothness of the wall. The hopper is classed as steep if the solids slide on it, and this is met by the following test. The hopper is steep if

$$\tan\beta < \frac{1-K}{2\mu_{\mathrm{h}}} \tag{3.31}$$

where $\mu_{\mathrm{h}}$ is the full wall friction coefficient on the hopper, which may have a lining. This relationship is plotted in Figure 3.10a for clarity. The effect of steepness on the pattern of pressures in hoppers during emptying of the silo is illustrated in Figure 3.10b.

However, the most critical feature of a hopper is not the wall pressure distribution but the overall equilibrium shown in Figure 3.8. Most structural failures of hoppers occur by rupture at the transition under the stress resultant $n_\phi$. High values of $n_\phi$ are chiefly caused by an excessive vertical pressure $q_{\mathrm{t}}$ from the cylinder, probably when this is underestimated through inadequate attention to material variability (Section 3.3.6).

### 3.3.5 *Simple structural concepts for cylinders*

The chief goal of predicting pressures in silos is to ensure the safety of the structure. So the effect of the pressure on the structure must be a key element. All early studies of pressures assumed that the simple equilibrium between normal pressure and hoop (circumferential)

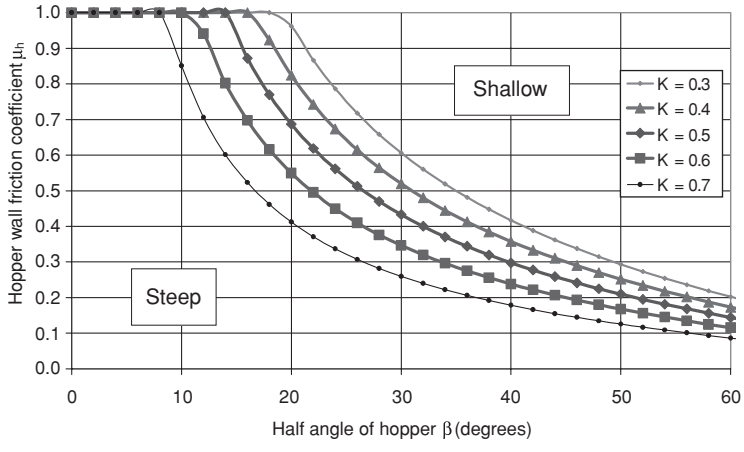


(a) Test for whether a hopper will be steep or shallow

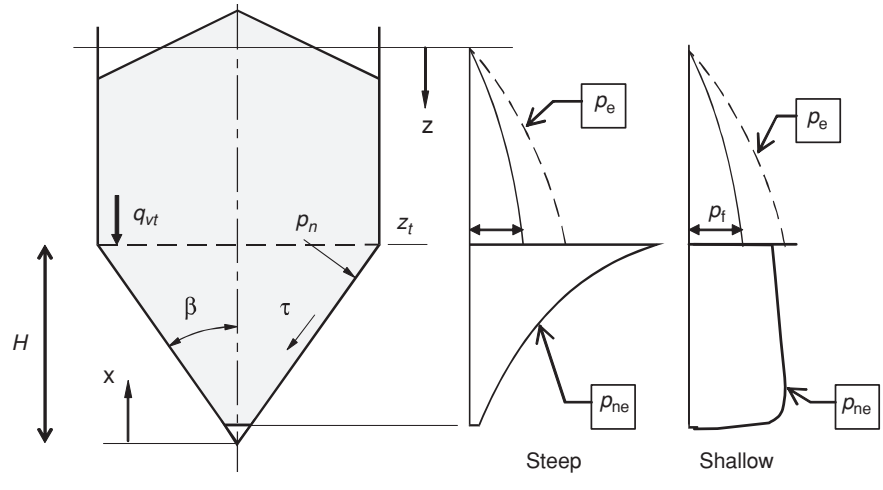


(b) Typical emptying pressure patterns in steep and shallow hoppers

**Figure 3.10** Steepness criterion and typical hopper pressures.

tension in the wall (Figure 3.11) was all that needed to be considered, leading to

$$n_\theta = pR \quad \text{for a circular silo} \tag{3.32}$$

where $n_\theta$ is the circumferential force per unit height in the wall. This equation is valid if the pressures are constant around the perimeter at any level in the silo. It indicates that higher pressures will lead to higher tensions and so presumably will be more damaging to the silo wall. This over-simplified concept has underlain much of the pressure values reported from silo research in the last century, and is certainly responsible for some failures which occurred when pressures dropped locally (see Section 3.4.5). The maximum pressure,

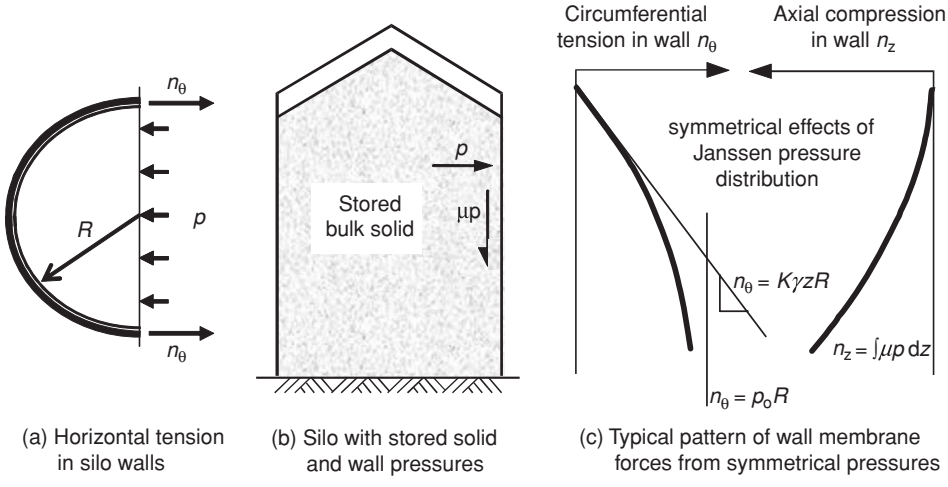


**Figure 3.11** Simple structural effect of symmetrical pressures.

especially if local and of short duration, is not usually a prime cause of structural damage to silos.

Accompanying the pressure $p$ against the wall is the frictional traction $\tau$ (Figure 3.4), which accumulates to produce vertical (axial) forces in the silo wall. Since the vertical pressure in the solid reaches an asymptotic limit (Equation (3.8)), the weight of all the additional solids must be borne instead by vertical forces in the wall (Figure 3.11c).

Adopting Janssen's theory for the pressure pattern, the resulting axial force per unit circumference $n_z$ developing in the silo wall under symmetrical conditions is then

$$n_z = \int_0^z \tau \mathrm{d}z = \int_0^z \mu p \mathrm{d}z = \int_0^z \mu p_0 (1 - e^{-z/z_0}) \, \mathrm{d}z = \mu p_0 z_0 \left( \frac{z}{z_0} - 1 + e^{-z/z_0} \right) \quad (3.33)$$

This compressive force rapidly approaches a linear increase with depth (term $z/z_0$) (Figure 3.11c). Thus very high forces develop in the wall towards the bottom of the silo. This force is important in thin metal silos, as it becomes the critical effect because the controlling design consideration is buckling under axial compression (see Section 3.5.2). This is the reason why metal silos must have a much greater wall thickness towards the bottom than near the top.

The above theory for cylinders is not valid for conical hoppers. For them, even the simplest stress analysis is much more complicated and is beyond the scope of this chapter. More information may be found in Rotter (2001a).

In reading what follows it should be noted that metal silos are most sensitive to vertical compression in the vertical walls, that concrete silos are most sensitive to normal pressures against the walls, and that both of these structural materials are easily damaged by unsymmetrical pressures, as noted in Sections 3.4.5 and 3.5. Finally, the hopper, which has not been discussed yet, is usually chiefly loaded by the vertical stress in the solid at the transition. These different sensitivities demand that careful attention is paid to different parts of the pressure theory, since it is not normal wall pressures alone that cause structural failures.

### 3.3.6 *Variability of the properties of stored solids*

The above theories are based on known properties of the stored bulk solid. However, industrial bulk solids have properties that vary considerably from time to time and from source to source. The extent of variability that a particular silo may see depends very much on its location: the solids in a silo that is part of a manufacturing process may vary rather little, whilst those at a mine or port facility are likely to vary considerably from year to year. Unfortunately, these differences cannot yet be accounted for in the design process, especially as the handling properties of solids often vary considerably when other properties (e.g. chemical composition) do not. Such changes can arise from moisture content, particle shape or surface roughness changes, traces of foreign materials and minor attrition during handling. Thus, it is wise to design all silos for the full range of properties that may arise.

In the world's first codified design rules (DIN 1055-6 1964), it was unstated, but tacitly assumed, that the silo was tall and made of concrete. Consequently, it was thought that the worst condition was normal pressures against the wall, and that a design would be safe if designed for the bulk solid that produced the highest pressures. Examining Janssen's equation (Equation (3.6)), it can be seen that these pressures are highest when the wall friction is low and the lateral pressure ratio is high. As a result, older tables of material properties, set out in standards, gave a single value of each property and tended to exaggerate the lateral pressure ratio $K$ and underestimate the wall friction $\mu$.

As metal silos have become much more common, the importance of vertical forces in the wall has become clear. These forces are largest when the solid has a high lateral pressure ratio $K$ and a high wall friction $\mu$. Thus, the single values of properties in old tables were not safe in design, and the standards were modified by adding an additional factor to the vertical force developing in the wall. In the same way, the total load on a hopper is greatest when the vertical force in the vertical wall is smallest, which occurs with a low lateral pressure ratio $K$ and low wall friction $\mu$. This was also accommodated in early standards by increasing the bottom force by a factor to allow a single value of each material property to be used.

Now that more potential failure modes in silos are understood, and the differing variability of different stored solids is appreciated, it is appropriate to try to define the upper and lower limits of each property value. As a result, most of the empirical additional factors can be removed from the design process, and safe design for specifically defined different extreme materials can be undertaken instead. In EN 1991-4 (2007), a central value for each property is listed, and it is then either multiplied or divided by a 'conversion factor' $a$ to achieve upper and lower extremes. The conversion factor represents the scatter of values that particular solid may display.

The extreme values of particular properties are termed 'characteristic values' in structural design and are intended to correspond to a 10% or 90% probability of occurrence. The characteristic values that should be used in structural design calculations are shown in Table 3.1 (taken from Rotter 2001a).

Most standards for silo structural design (AS 3774 1996; DIN 1055-6 2006; EN 1991-4 2007) now acknowledge the variability of the properties of bulk solids and permit the variability of each solid in its own setting to be determined by testing. A formal methodology for establishing the variability of a given solid is given in Annex C of EN 1991-4 (2007).

**Table 3.1** Values of properties for different wall loading assessments.

| | Characteristic value to be adopted | | |
|---|---|---|---|
| Purpose: | Wall friction coefficient ($\mu$) | Lateral pressure ratio ($K$) | Angle of internal friction ($\phi_i$) |
| For the vertical wall or barrel | | | |
| Maximum normal pressure on vertical wall | Lower | Upper | Lower |
| Maximum frictional traction on vertical wall | Upper | Upper | Lower |
| Maximum vertical load on hopper or silo bottom | Lower | Lower | Upper |
| Purpose: | Wall friction coefficient ($\mu$) | Hopper pressure ratio ($F$) | Angle of internal friction ($\phi_i$) |
| For the hopper wall | | | |
| Maximum hopper pressures on filling | Lower value for hopper | Lower | Lower |
| Maximum hopper pressures on discharge | Lower value for hopper | Upper | Upper |

*Note 1:* It should be noted that $\phi_{wh} \leq \phi_i$ always, since the material will rupture internally if slip at the wall contact demands a greater shear stress than the internal friction can sustain. This means that, in all evaluations, the wall friction coefficient should not be taken as greater than $\tan\phi_i$ (i.e. $\mu = \tan\phi_w \leq \tan\phi_i$ always).
*Note 2:* Hopper normal pressure $p_n$ is usually maximised if the hopper wall friction is low because less of the total hopper load is then carried by wall friction. Care should be taken when choosing which property extreme to use for the hopper wall friction to ensure that the structural consequences are fully explored (i.e. whether friction or normal pressures should be maximised depends on the kind of structural failure mode that is being considered).

## 3.4 Pressure changes during discharge of solids (emptying)

### 3.4.1 *First discoveries and explanations*

In some of the earliest experiments (Ketchum 1907) it was discovered that the pressures often increased when the silo was emptied. The increase was not often to a fixed value, but the pressures tended to rise and fall with time. Increases ranged from perhaps 10 to 30% as stable values, whilst very short-term local rises were seen to perhaps 2 or 3 times the Janssen value. Since the concept being used was that the Janssen theory gave the first measure of silo effects, it was natural to think that there was a 'pressure' at every level, so that this single pressure could be measured using a single pressure cell. Thus, the high pressures were imagined to occur as symmetrical high pressures at every point where they were observed.

Some effort went into trying to understand why these high pressures might occur, but the key idea came from Nanninga (1956) who suggested that the solid was in an active Rankine state after filling (higher vertical pressures than horizontal) and that during emptying it must be in a passive state (declining vertical pressures whilst the horizontal ones were retained). The transition between these two states would lead to a rapid increase in the value of $K$, whilst the vertical stress, in equilibrium across this change, would remain constant.

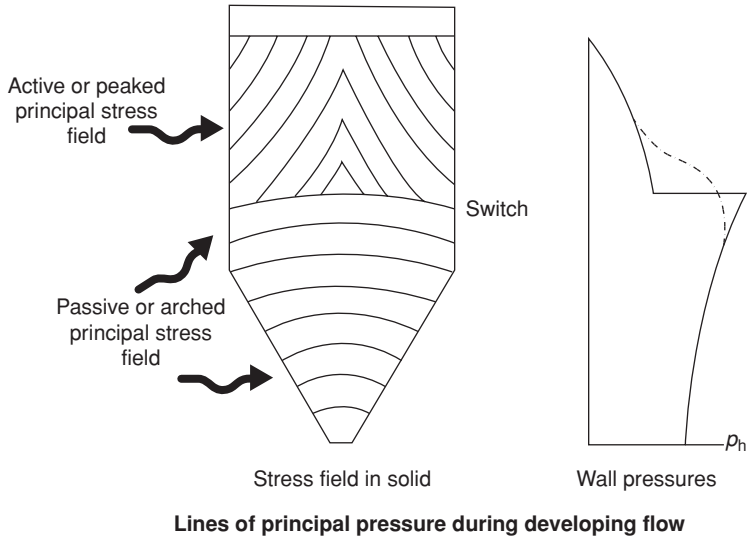


**Figure 3.12** Original concept of the 'switch' during emptying. (After Gaylord & Gaylord 1984.)

Nanninga (1956) suggested that the changeover might occur over a finite depth (Figure 3.12), but later theorists who took up the idea (Arnold & McLean 1976; Jenike *et al*. 1973; Walker 1966; Walters 1973) made the change into an abrupt step. This step was termed the 'switch'.

Since the state was to pass from filling (close to an active stress state) to passive, the pressure just below an abrupt step is easily determined as the Janssen value multiplied by the ratio of passive to filling values of lateral pressure ratio ($K_p/K_f$). The ratio of peak symmetrical discharge pressure to symmetrical filling pressure is a very widely used variable, and its origins can be seen here to have some foundation in mechanics. This ratio is so important in silo design that it is given a symbol and defined as

$$C_e = \frac{p_e}{p_f} \tag{3.34}$$

in which $p_f$ is the normal wall pressure after filling and during storage (taken as the Janssen pressure) and $p_e$ is the design value of the symmetrical pressure (uniform at a given height in the silo) occurring during emptying (discharge). The above description leads to $C_e = K_p/K_f$.

It was noted above that the ratio $K_p/K_a$ for a typical bulk solid is of the order of 9, making $K_p/K_f$ of the order of 6. No observations of such huge increases in pressure were ever reported, so several theories were advanced which tried to explain why the switch from active to passive could produce lesser increases in pressure. The revised theories (Arnold *et al.* 1980; Jenike *et al.* 1973; Walker 1966; Walters 1973) showed that the stress pattern in the solid, involving non-uniform vertical stresses and shear stresses against the wall, could lead to rather smaller wall pressure increases. The Walker and Walters treatments relied on the solid being in a fully plastic (yielding in shear) state at all times, whilst the Jenike treatment assumed that it was elastic. Typical examples of the resulting pattern of wall

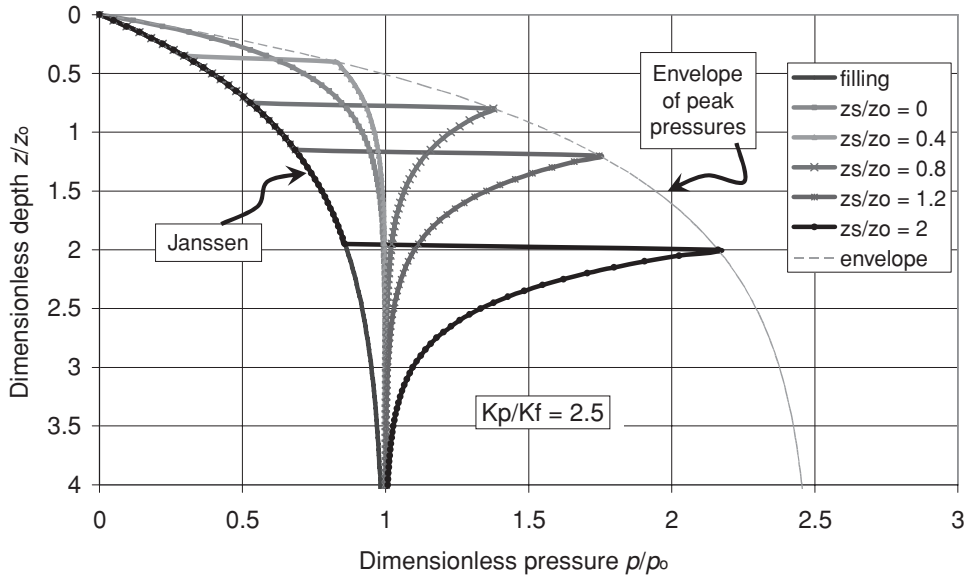


**Figure 3.13** Consequences of a 'switch' in lateral pressure ratio at different levels (the switch is taken to occur at depth $z_s$).

pressures are shown in Figure 3.13, where it is supposed that the ratio $K_p/K_f$ is only 2.5. Conventional wisdom, following the simple structural theory set out in Section 3.3.5, said that the design must accommodate the envelope of pressures corresponding to the maximum pressure applied at every level.

All these attempts still led to large predicted pressure increases during emptying, and for a while it was accepted that very large increases in symmetrical wall pressures must occur and should be designed for. A strange aspect of this idea was that, although many silo failures did occur, few silos failed by bursting, which is what would have been expected if the theories were accurate.

It may be noted that the pressure always returns to the Janssen asymptotic value $p_0$ below the 'switch'. The increase in the axial force developing in the wall is much smaller (Figure 3.14) because the switch only affects the frictional shear transfer locally.

The most widely used switch theory for vertical walls was that of Jenike *et al.* (1973), which still underlies the flow pressure rules in the Australian Standard AS 3774 (1996), leading to a high ratio of design pressures for discharge to those after filling. This type of theory is still commonly expounded (Drescher 1991) as a formal part of silo pressure behaviour.

### 3.4.2 *A better understanding*

The chief difficulty with the switch theory is its abrupt change from the filling pressure ratio to the discharge value. If a smoother change, based on test data in $K_0$ tests on solids, is used (Rotter 1999), much smaller rises in symmetrical pressure are found as the peak is

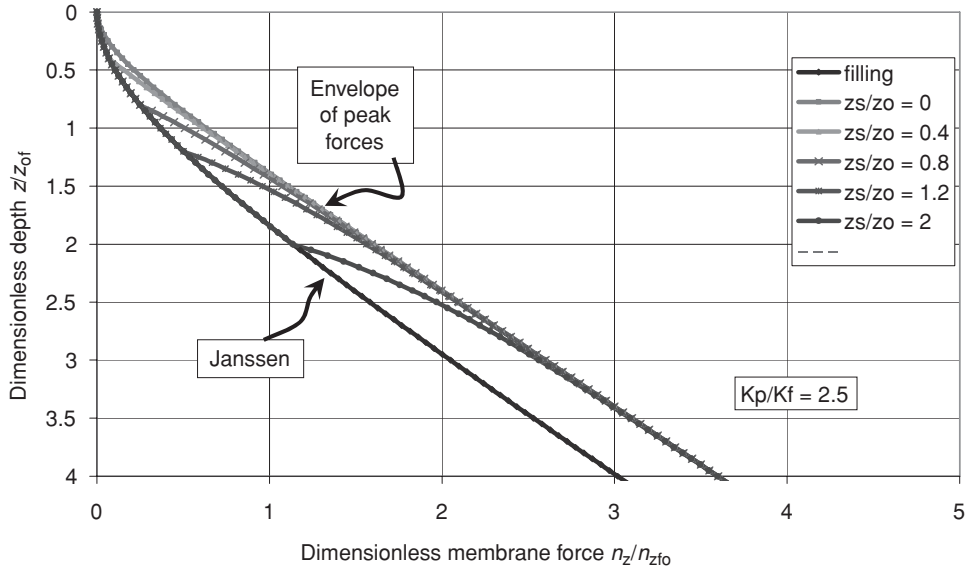


**Figure 3.14** Smaller rises in the vertical force in the wall beneath a 'switch'.

rounded by the slow change (Figure 3.15). Here a progressive change in $K$ from $K_f = 0.5$ to $K_e = 1.4$ (a ratio of $K_e/K_f = 2.8$) is assumed to occur between the heights $z/z_0 = 0.6$ and 0.75. The resulting changes in the mean vertical stress $q/q_0$, the mean wall pressure $p/p_0$ and the emptying factor $C_e$ are shown in Figure 3.15 with the assumed ratio $K/K_f$ at each level. Because the change is progressive (as originally suggested by Nanninga), the rise in pressure from filling to emptying is only a factor of 1.5 instead of 2.8 (i.e. the step change greatly exaggerated this phenomenon). The same analysis yields similar results for different locations of this change and thus leads to the conclusion that, although the stress field must undoubtedly change from the filling to emptying states, the magnitude of the symmetrical rise in pressure is greatly overpredicted by these simple switch theories. The European Standard (EN 1991-4 2007) consequently prescribes much smaller increases in symmetrical pressure during emptying ($C_e$ values) than these older theories propose.

### 3.4.3 *Pressure observations during emptying*

Many experiments have been conducted to explore the pressures on silo walls during emptying. The data from these experiments are extremely voluminous: it is difficult for researchers to report very large quantities of data in publications. As a result, only what is judged to be the most important information is documented. A huge experimental programme on many different solids was conducted by Pieper and his team (Pieper & Wenzel 1964) in Braunschweig, and much of the following comes from their work. Unfortunately, some simplifications that they used, appropriate at that time, have been used by others for much longer than they might have wished.

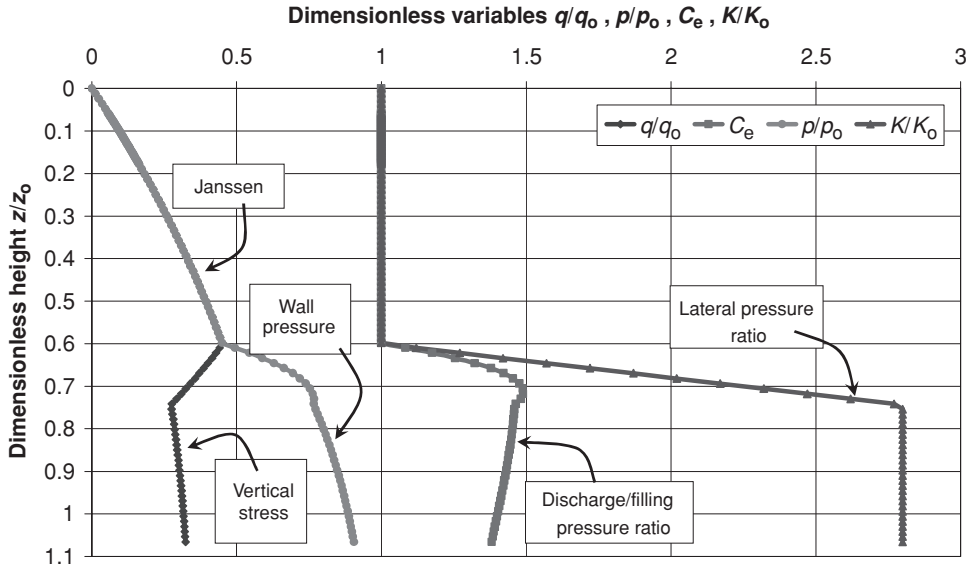


**Figure 3.15** Effect on pressures of a smooth change in lateral pressure ratio.

A typical set of observations from pressure cells on the side of a tall silo subject to concentric filling and discharge and containing sand is shown in Figure 3.16, where the pressure reading is plotted against time during the test.

The lowest pressure cell, A, is the first to register pressure (at 2 min), and the pressure rises rapidly towards the Janssen asymptote. The other cells progressively start to register

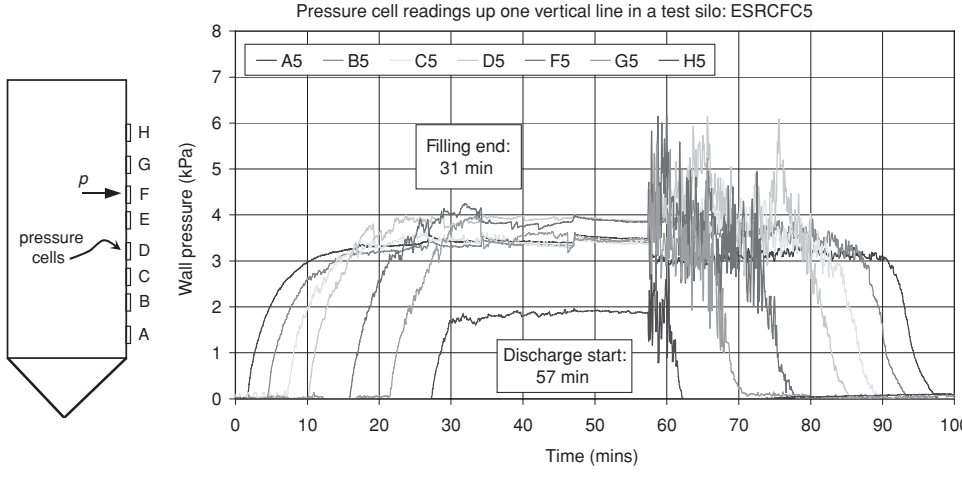


**Figure 3.16** Typical pressure cell record on a vertical line of cells in a test silo.

as the silo is filled past the level they are at. It is interesting to note that at the end of filling (31 min) the pressures are not in a neat order with the lowest cell registering the highest pressure, but a little jumbled, indicating that the Janssen theory is not a precise tool like pressures in a fluid vessel, but an approximate description. After the filling process ends, the pressures are relatively stable, but not completely constant because small settlements and minor disturbances cause small increases and decreases in different places at different times.

At the instant that the discharge gate is opened (57 min) all the pressure cells begin to fluctuate quite wildly, with pressures rising for short moments to as much as twice the filling value but also falling to very low values. The largest departures from the filling state occur relatively high up the silo wall at levels D and F with the cell at F once touching 6.2 kPa from a Janssen reference value of 3.6 kPa (ratio of 1.7). But there is no evidence of a wave of high pressure passing up the silo as the stress field passes from filling to passive, and the switch theory of silo pressures on vertical walls, at least in its original form, is probably not widely believed any more.

Many silo pressure researchers, when faced with such voluminous data as this which is clearly not easily assimilated, have tried to find values that can be reported as relevant to the discharge condition, and it is quite natural that the highest pressure occurring on each pressure cell should be reported, irrespective of whether these values occurred simultaneously and whether they endured very long. Thus, the literature has many reports of major departures from the filling state, but the significance of these departures is highly questionable. The classic interpretation process is illustrated in Figure 3.17, where different cells reach peak pressures at different instants, the envelope of these peak pressures is represented as the outcome of the test, and a Janssen envelope is fitted to cover the outcome so that the result can be reduced to a single overpressure factor $C_e$. Alternatively, revised values of $K$ and $\mu$ could be given to represent the emptying process (e.g. DIN 1055-6 1964). Many of the difficulties with such simplified interpretations were discussed by Rotter *et al.* (1986): in particular, the most damaging instant for the silo structure is not detected or encompassed by this process.

One must not be too unkind to the researchers who reported these experiments. The instrumentation is very expensive, so most tests were conducted with relatively few pressure cells. Faced with the challenge of where to place their few cells, most experimentalists were persuaded by the above theories that placement down a vertical line on the side of the silo would deliver the pattern of pressure to be expected, naturally a constant value at each level. Consequently, the information concerning variation of pressure at a particular level is rather sparse.

A further reason for using only one pressure cell at each level was that the simple theory used to translate pressures into forces in the structure (Equations (3.9) and (3.10)) implied that only the largest pressure needed to be found, and presumably that large pressure might well pass by every point at a particular level, even if not quite simultaneously.

The pressures recorded at different points around the circumference in the same test as in Figure 3.16 are shown for one level in Figure 3.18. First, it is clear that the pressures after filling are not at quite the same value at one level. Second, the rises and falls in pressure at different points around the circumference are not coincident, but lead to significantly unsymmetrical patterns at different instants. A detail taken from Figure 3.18 is shown in Figure 3.19.

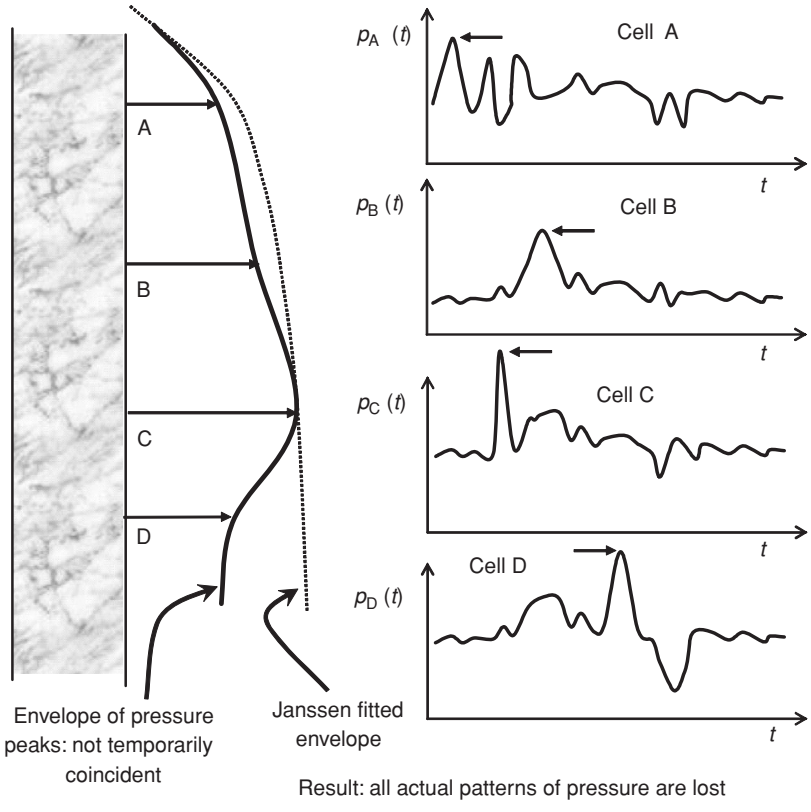


**Figure 3.17** Typical interpretation process applied to pressure observations.

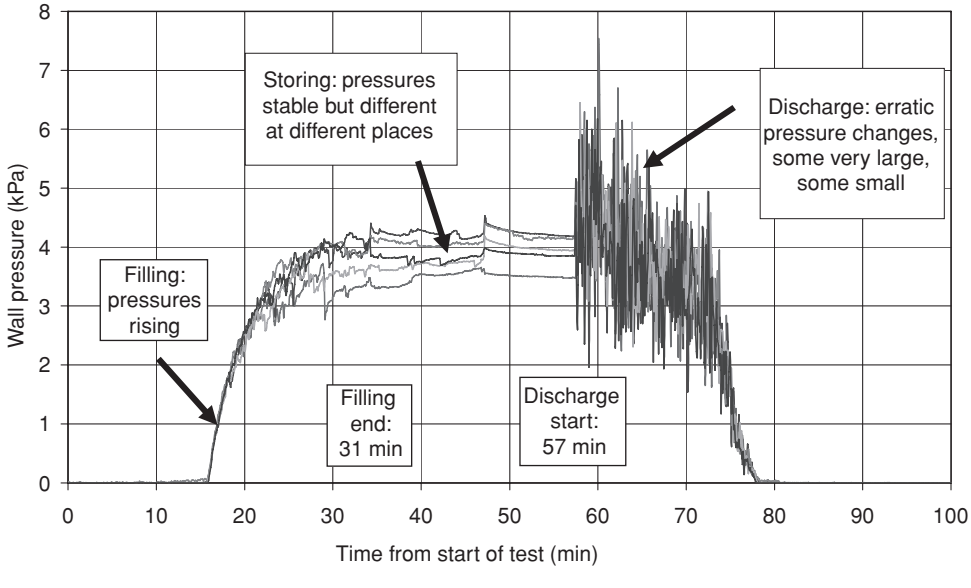


**Figure 3.18** Typical pressure cell record at a single level in a test silo.

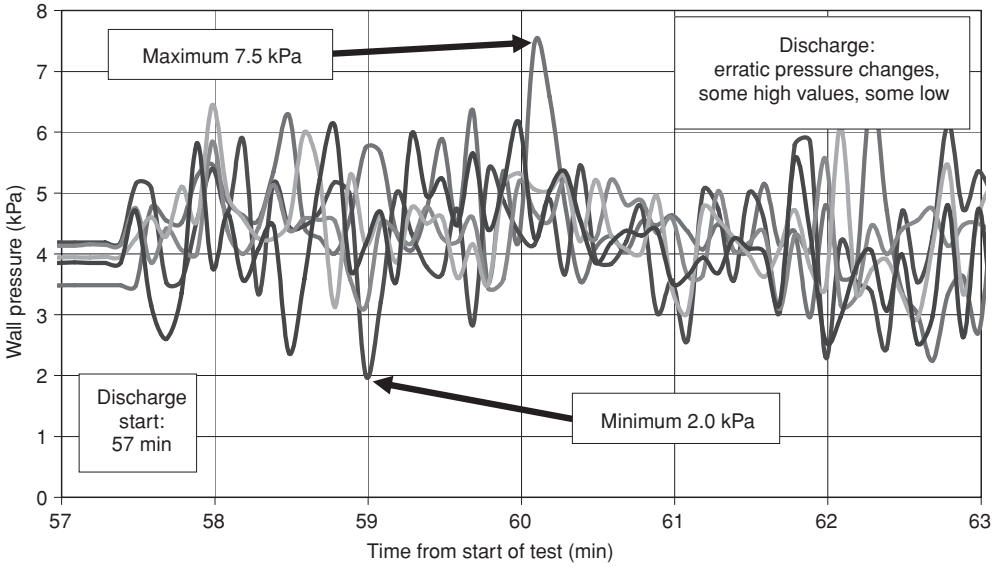


**Figure 3.19** Detail of Figure 3.18 showing local rises and falls in pressure.

The key factor here is that unsymmetrical pressures are often damaging to cylindrical silo structures, whether constructed in metal or concrete, and this effect is more important than the possible peak pressure occurring at one point. In particular, if the peak pressure only occurs at one point around the circumference, then the pressures are necessarily unsymmetrical and the worst aspect of this load case is not the simple relationship between normal pressure and circumferential (hoop) tension of Figure 3.11.

In the context of the above, a key set of experiments on full-scale silos was conducted in Sweden over many years (1970–1980) by Nielsen and his co-workers (Nielsen 1998). This project arose because of the extensive cracking which had been observed in many Swedish grain silos. The experiments involved a 47 m high concrete silo of internal diameter 7 m, filled with different grains in different experiments with both concentric and eccentric filling and discharge. This huge set of experiments demonstrated many effects that are not included in any silo design, notably the progressive changes in the properties of the stored solid as it was handled, the sensitivity of pressures to anisotropic packing of the particles, the effects of imperfections in the silo walls, the difficulty of making reliable observations with pressure cells, and the fact that two pressure cells close to each other might, for limited periods, record quite different values, indicating that there can be sharp jumps in pressure on the wall.

The most critical finding for silo design was the systematic pattern of unsymmetrical pressures, both after filling and during discharge (Ooi *et al.* 1990). The ratio of the largest sustained pressure to the smallest at a single level could be as high as 2.8 under static conditions after filling and 5.6 during discharge. This kind of discovery was also made by Schmidt and Stiglat (1987) and led to the introduction of a required unsymmetrical design

pressure, called a 'patch load' in the German standard (DIN 1055-6 1987). The latest version of this patch load treatment is given in EN 1991-4 (2007) where the patch load depends on the filling or discharge state, the silo aspect ratio, the eccentricities of filling and discharge and the construction medium.

The consequences of unsymmetrical pressure patterns are noted further in Section 3.5.

### 3.4.4 *The importance of flow patterns during discharge*

The discussion above concerning pressures during emptying has omitted a key aspect that became very clear during the 1960s and 1970s. The manner in which a solid flows within the silo has a major effect on the pressures exerted on the silo wall.

If the entire mass of solid in the silo is in motion, then it slides against the wall, producing the effect seen in Figures 3.16, 3.18 and 3.19, and the local pressure can be much influenced by variations in the straightness of the wall and its local roughness. By contrast, when the solid against the wall is at rest, the pressures generally remain close to the Janssen filling values. The work of Jenike (1961, 1964) was probably the main driver towards explicit recognition of the importance of 'flow pattern' of the solid. A modern description (EN 1991-4 2007) divides the possible flow patterns into three main categories under symmetrical conditions (Figure 3.20).

These images show an idealised version of the pattern of flow. The real boundaries of flow channels often vary a little from time to time because they depend quite sensitively on small changes in the packing of particles (Arnold 1991). Further, the idealised pattern is shown with the silo completely full, but the pattern cannot develop until some solid has come out at the bottom (unless it is being continuously replenished). However, because the critical design condition is almost always when the silo is full, this is the idealised reference shape.

Following the work of Jenike (1961, 1964), it is possible to determine with reasonable precision whether the silo will exhibit mass flow or funnel flow. The conventional diagram is similar to that for hopper steepness and shows the boundary between mass flow and funnel flow (Figure 3.21) as a function of the hopper slope and wall friction coefficient. There are similar diagrams for wedge hoppers, for which mass flow is more easily achieved (EN 1991-4 2007; Rotter 2001a). This figure marks the mass flow zone as a 'risk' because the hopper pressures may be high only in this case. The boundary distinguishes between mass flow and other types of flow: it does not distinguish pipe flow from mixed flow, and this is one of the most serious current problems in silo pressure prediction. Unfortunately, there is, as yet, no reliable method of determining the shape of a mixed flow channel, or of reliably determining when it may strike the wall at an effective transition (Figure 3.20c).

The typical patterns of symmetrical pressure against the wall for the three simple patterns of flow are shown in Figure 3.22. Under mass flow (Figure 3.22a), the high pressure that develops at the top of the hopper (sometimes referred to as 'the switch') is caused by a high $F$ (Figure 3.9), associated with the solid below this point being in a passive stress state. Much has been made of this high local pressure, but structural research studies have shown that it is not critical to the strength of metal silos, and is indeed beneficial (Rotter 1986a; Teng & Rotter 1991).

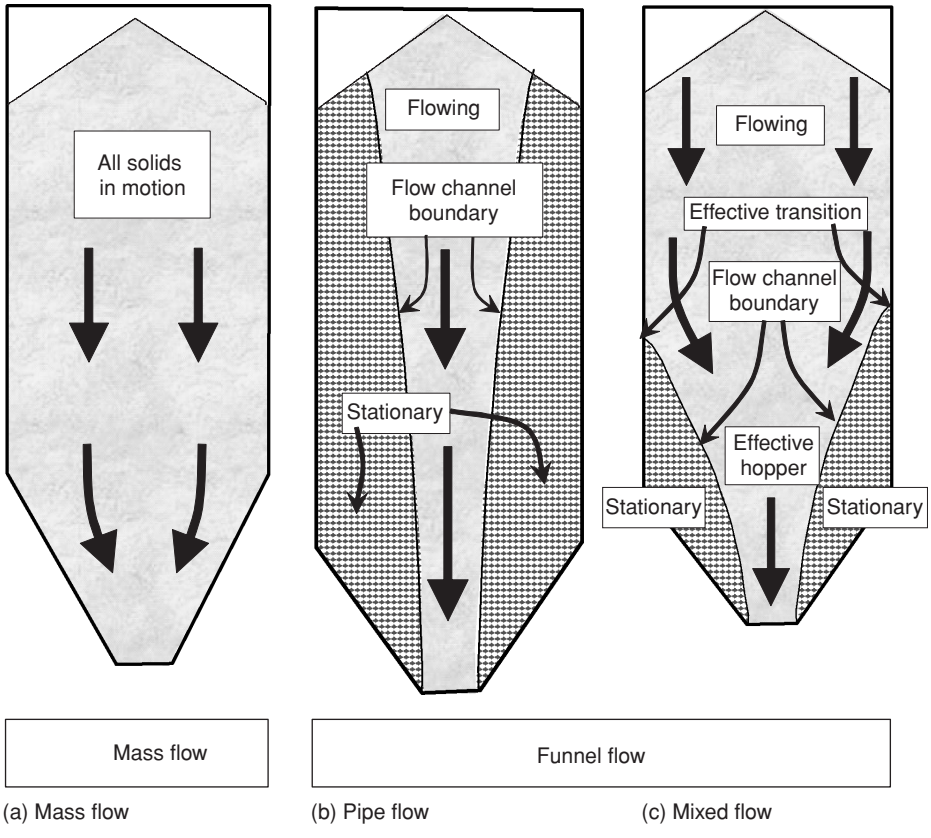


**Figure 3.20** Chief categories of symmetrical flow pattern.

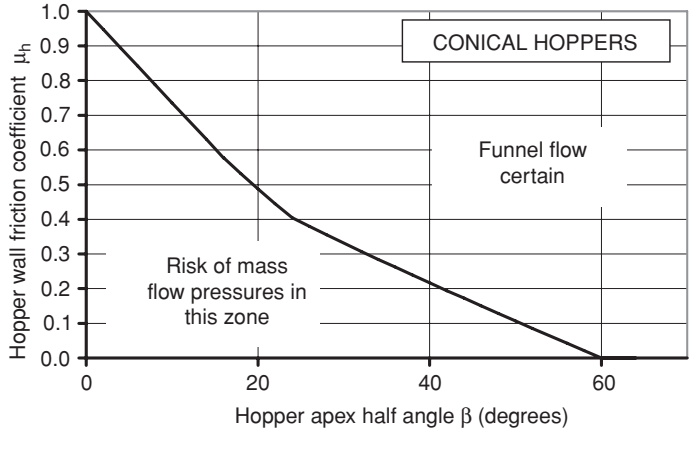


**Figure 3.21** Boundary between mass flow and funnel flow in silos with conical hoppers. (After EN 1991-4 2007.)

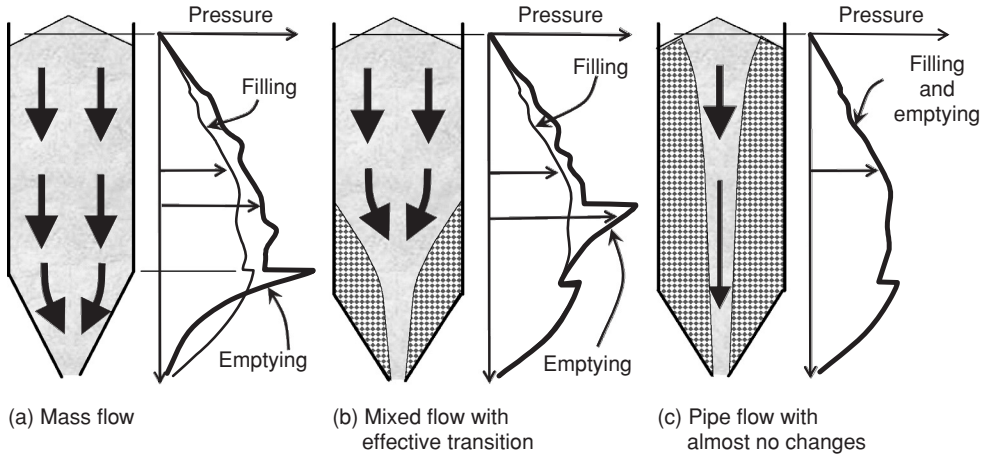


**Figure 3.22** Typical patterns of average symmetric wall pressure after filling and during emptying, for different flow channel geometries.

Under pipe flow (Figure 3.22c), the pressures against the wall are largely unaffected by flow, so if the designer can be sure that no flow of solids against the wall will occur (except at the surface), lower design pressures are possible. However, under mixed flow (Figure 3.22b), the boundary of the flow channel strikes the wall and a local high pressure, comparable to that in a mass flow hopper, often develops against the wall. This pressure is somewhat unpredictable. It can vary in magnitude as the slope of the contact point changes, it can be unsymmetrical from one side to the other, it is slightly cushioned by the stored solid between the flowing solid and the wall, and in silo experiments, this is commonly the point of greatest scatter and oscillation in pressure values. Despite all of this, very few silos have ever failed by bursting at an effective transition, so this rather alarming knowledge should not be a major cause for concern.

Finally, it must be clearly repeated that it is not yet possible to predict the geometries of pipe flow and mixed flow solids flow patterns, so this rather critical distinction is not yet quantifiable. The distinction is therefore not used in the design rules of EN 1991-4 (2007).

### 3.4.5 *Eccentric discharge and its consequences*

The most damaging condition for most silos is the unplanned occurrence of unsymmetrical flow regimes, if the flow channel makes contact with the silo wall. This is conventionally referred to as eccentric discharge. It has caused so many silo disasters that many writers have proposed that it should never be used. But two situations arise: it may be necessary to have off-centre discharge outlets for functional reasons, and conditions in the silo (blockage of feeders, uneven thermal or moisture conditions, segregation of contents etc.) may cause unintended eccentric flow. There are numerous causes of such eccentricities.

This is a substantial subject and beyond the scope of this chapter, but EN 1991-4 now includes a simple definition of a design eccentric flow channel geometry and pressure regime which may be used to achieve a satisfactory design. The equations used adopt the theory of Rotter (1986b, 2001b). A circular silo with a part-circular flow channel in contact with the wall (Chen *et al.* 2005) is shown in Figure 3.23, together with the characteristic pressure distribution that is found in experiments. The vertical stresses induced in the wall by this unsymmetrical pattern are also shown to indicate the dramatically large effect on this silo. In particular, note that the highest compression stress occurs around the mid-height of the silo in the middle of the flowing channel.

Eccentric discharge pressures of the pattern shown in Figure 3.23 also have a very damaging effect on concrete silos, where severe bending of the wall induces substantial vertical cracks and sometimes leads to spalling.

## 3.5 Structural damage and its causes

### 3.5.1 *Introduction*

The simplest stress analysis of a cylindrical silo structure under symmetrical loads was presented above in Section 3.3.5. Unfortunately, this is often the only analysis that is applied, sometimes with unfortunate consequences for the structure. Metal and concrete silos carry their loads differently because metals are strong in tension but thin metal sections tend to buckle under compression. By contrast, concrete is very weak in tension, but can resist compression well. These aspects lead to different key design considerations.

Both metal and concrete silos are thin shell structures. Shell structures have more complex patterns of behaviour than any other structural form, they are more sensitive to small errors of geometry and they have more possible failure modes. As a result, it is common for designers to oversimplify the problem, and especially to misdiagnose the cause of structural damage. The subject is very large and only a brief outline is given here. More information may be found in Rotter (2001a) together with the Eurocodes on metal silos (EN 1993-4-1 2007) and shells (EN 1993-1-6 2007).

Shell structures tend to suffer serious effects when the pressure is not uniform at one level. A local drop of pressure can cause serious damage, of different kinds, in both metal and concrete structures. Where signs of damage are seen, possible causes of loss of symmetry should be the natural first investigation path to follow.

### 3.5.2 *Steel and aluminium silos*

3.5.2.1 *Bolted and welded construction* A first distinction must be made according to the form of joint that is used in metal silo construction. Many smaller steel silos have bolted joints, and where these are present, every stress developing in the wall, at every point, must be transmitted through a joint. The joints are lines of weakness, so they should be made stronger than is strictly necessary. Careful attention should be paid to edge distances, and it is most desirable that the weakest failure mode of the joint should be by bearing rather than bolt shear, since the latter is not very ductile and lack of fit in the joints may cause

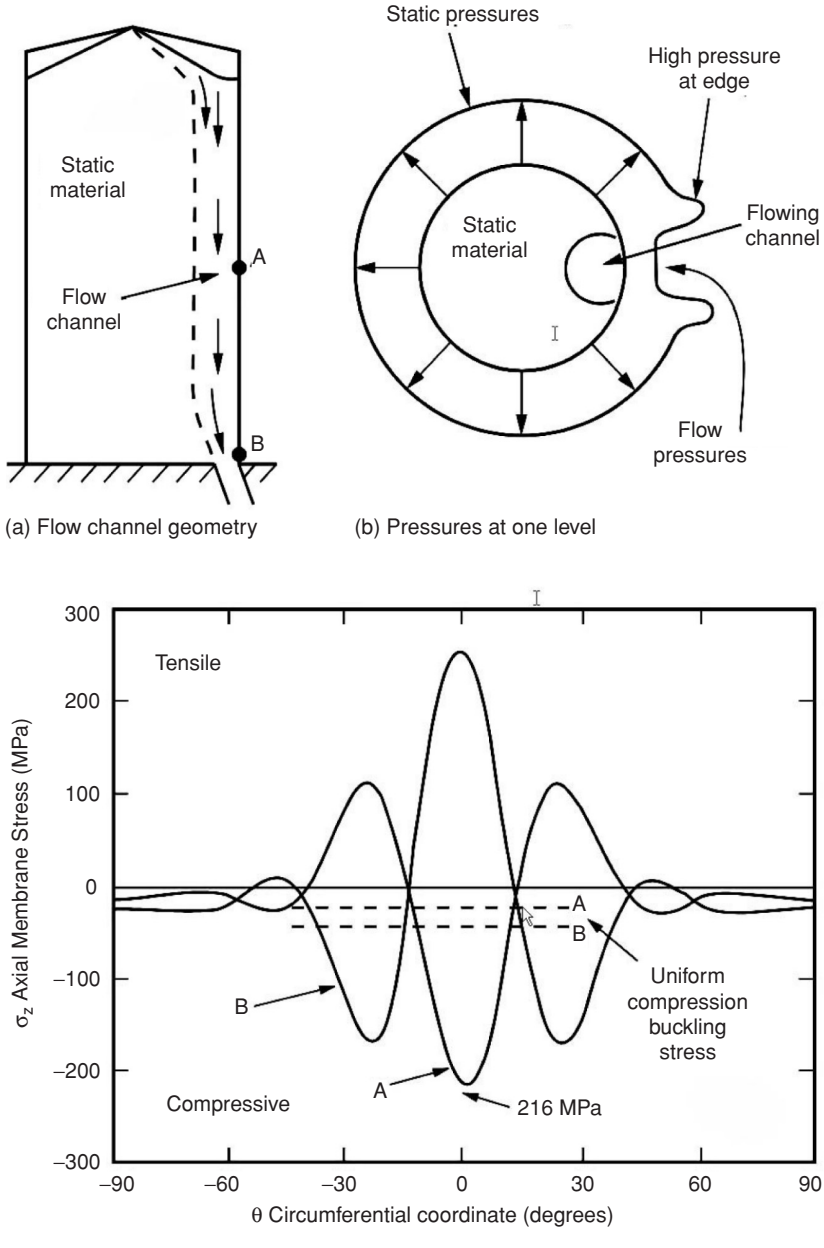


(a) Flow channel geometry

(b) Pressures at one level

(c) Varying vertical stress around perimeter at A and B (compare symmetric loading value)

**Figure 3.23** Flow channel geometry, typical pressure pattern and vertical wall stresses during eccentric discharge.

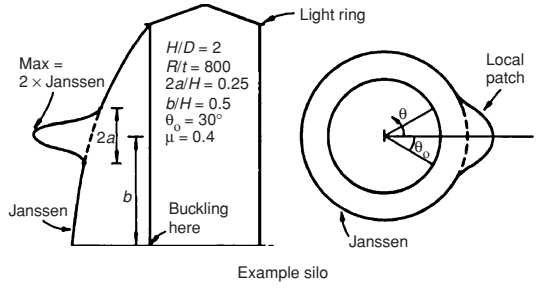


(a) Example silo with patch of high pressure

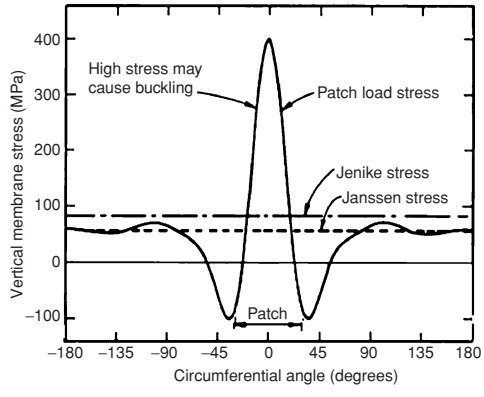


(b) Vertical stresses induced in wall

**Figure 3.24** Stresses resulting from a patch of normal pressure on a thin silo.

unzipping of a complete joint from a single zone of slightly elevated pressure. Larger bolts in thin plates are more ductile than smaller bolts in thick plates. None of these problems arises in welded construction.

3.5.2.2 *Bursting of the vertical wall* Bursting failures are very uncommon and are almost all found in bolted silos where a joint detail has failed. A careful analysis of the loads and strengths in different modes shows that this failure mode is only critical near the surface, or in squat silos.

3.5.2.3 *Axial compression buckling of the vertical wall* Buckling of the vertical wall is by far the commonest failure mode in metal silos. The buckles can be huge or quite local, but all buckles should be treated as very serious because this mode of failure is often dramatically catastrophic.

Axial compression arises from the friction transmitted to the silo wall by the solids. But axial compression also develops as a result of unsymmetrical pressures against the silo wall, caused by shell bending phenomena, which cannot be explained within the space limits here. An example is shown in Figure 3.24 where a local small patch of pressure on the silo wall induces high vertical compression (not due to friction) far from the patch. In particular, a

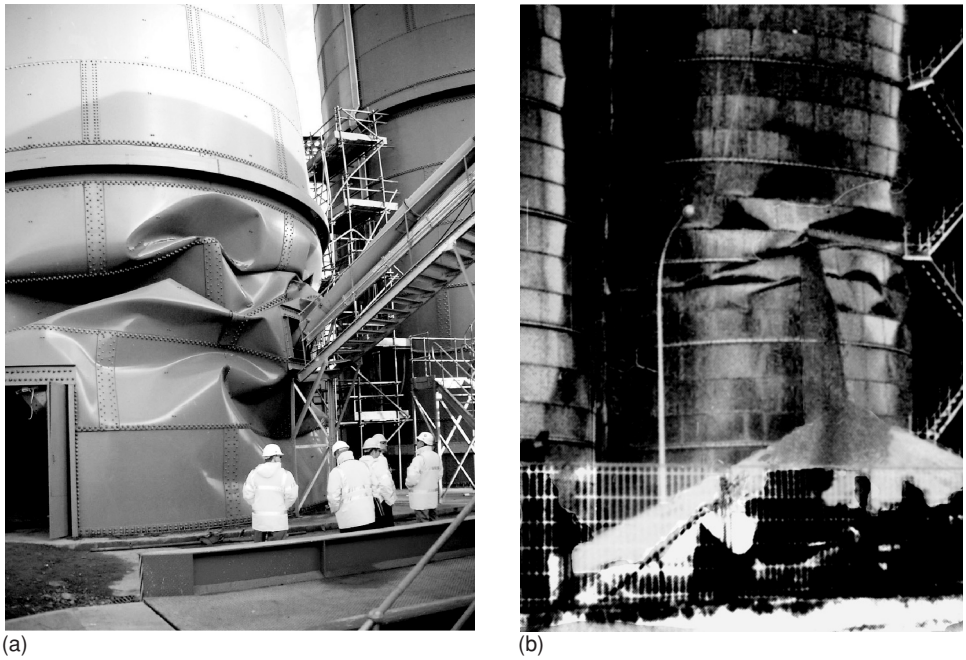

(a) (b)

**Figure 3.25** (a) Flyash silo with buckle arrested by hopper impacting the ground; (b) grain silo en route to total destruction as grain leaks from a buckled zone.

local loss of pressure can result in large increases in vertical compression stresses far above the point of pressure loss (Rotter *et al.* 2006). The location of the buckle is therefore not always a good guide to the location of the problem.

Buckling under axial compression occurs at very low stresses compared with the material strength (perhaps at 20 MPa in a metal with yield stress 250 MPa), and the strength is very sensitive to small errors of geometry. The post-buckling behaviour is also notoriously catastrophic. Two examples, where total destruction has not yet occurred, are shown in Figure 3.25. The buckles are relatively small, often with a characteristic diamond shape.

Under high internal pressures, a different form of axial compression buckle occurs, termed the 'elephant's foot' because of its smooth flat squashed shape. Also, where a buckle occurs adjacent to a support, a buckle may develop in the local high stress field, needing a more careful evaluation (the force being transmitted may not be easily determined).

3.5.2.4 *Eccentric discharge buckling of the vertical wall* A separate section is noted here for conditions of eccentric discharge. This is the commonest cause of axial compression buckles, where the low pressures against the wall in the flow channel cause high vertical compressive stresses over part of the perimeter near the mid-height of the silo (Figure 3.23). Extremely catastrophic failures are easily produced in tall silos, in which the whole silo falls over in the direction of the discharge outlet. The analysis of this problem can be found

in Rotter (1986b, 2001b). The condition is often mistaken as being caused by bending moments in the wall (Jenike 1967; Wood 1983), and these moments are indeed present, but bending does not produce diamond pattern buckles. The complex behaviour of cylindrical shells under unsymmetrical loads is, unfortunately, not widely understood.

The evaluation of the buckling strength under different conditions is quite complicated and can be found in Rotter (2001a), EN 1993-4-1 (2007) or EN 1993-1-6 (2007).

3.5.2.5 *External pressure buckling of the vertical wall* When a silo is empty, the thin wall is very susceptible to buckling under extreme wind. The buckles associated with this loading tend to be much larger than those for axial compression, usually stretching either the whole height of the silo or from a plate thickness change up to the top. Similar buckles occur when a partial vacuum is induced by the discharge of solids of low permeability and the silo is inadequately vented. For advice, see EN 1993-4-1 (2007).

3.5.2.6 *Shear buckling of the vertical wall* Where a squat silo (low aspect ratio) is either eccentrically filled (unsymmetrical top pile producing different heights of solid-wall contact) or is subjected to seismic excitation, the wall can buckle in shear near the foundation. These buckles have a characteristic diagonal stripe shape, but these load cases are relatively rare.

3.5.2.7 *Rupture, plastic deformations and buckling in hoppers* Hoppers made in bolted construction are susceptible to fracture of the joint at the point where the structural stresses are most seriously mismatched with the joint strength. The pattern of stresses is not the same as the pattern of pressures, but in bolted hoppers it is important to adopt a correct pressure pattern so that these joints are well designed. Once a failure initiates, unzipping tends to occur, leading to catastrophic failure.

In welded hoppers, failure is much less likely in the hopper itself. Most failures occur near the top of the hopper, and are either rupture (the hopper is torn off, with unzipping passing around the perimeter) or plastic deformations. Both situations arise from an excessive total load on the hopper or from unsymmetrical pressures, not from a high 'switch' pressure at the transition. For design and evaluation advice, see Rotter (2001a) and EN 1993-4-1 (2007).

3.5.2.8 *Buckling and yielding in transition rings* The transition is subject to high compressions because the hopper has a sloping form. Both buckling and yielding failures can occur in these rings, but these situations are usually caused by a misunderstanding of the complex stresses in such rings especially near supports (thrust, bending, torsion and shell flexure), rather than any special event in the stored bulk solid.

### 3.5.3 *Concrete silos*

3.5.3.1 *General* Concrete is good in compression, but cannot resist tensile stresses at all. Unfortunately, silos are essentially structures in tension, holding in the stored solid.

When concrete is subjected to tension, it cracks at right angles to the tension. It is normal to reinforce concrete to carry the tensile forces, but this reinforcement cannot carry stresses without stretching (strains), and this same stretching causes the concrete to crack. Cracked concrete often permits ingress of moisture and may lead to degradation of the stored product. The simplest solution is to prestress the concrete with steel high strength strand, so that it is in compression before any load comes on it. Then when additional tensile stresses are induced in the wall by the stored solid, they simply reduce the pre-existing compression.

Vertical compression does not usually cause problems in concrete silos since the weight of concrete, the thickness and the good compressive strength all contribute to excellent strength.

3.5.3.2 *Cracking under bending moments* The chief problem for concrete silos is cracking under bending moments induced by unsymmetrical pressures, where a zone of low pressure occurs inside the silo, the wall bends inwards, cracking on the inside (possibly not visible without careful inspection), possibly with adjacent regions of cracking on the outside at the edges of that zone. To prevent serious cracking of this kind, all concrete silo walls must be designed with some significant bending strength, and this is arranged by using an inner and an outer layer of reinforcement and requiring the design to support unsymmetrical loads. In EN 1991-4 (2007), 'patch' loads are defined on the silo wall which are intended to produce similar bending moments in the walls to those that would be produced by the real unsymmetrical pressure patterns discussed above. However, these patch loads have not yet been properly calibrated against the outcome of tests on silo pressures, so the design magnitude is not yet very certain.

Where concrete silos are subject to eccentric discharge, the low pressures in the flowing solid cause reduced pressures against a limited part of the wall, and the primary effect of these is to induce vertical cracks associated with circumferential bending. However, the concrete silo is a shell structure, albeit thicker than the metal silos, and eccentric discharge has been shown (Rotter 2001c) also to cause cracking in the roof and severe damage to internal structures simply because the effects of the flow channel low pressure are transmitted throughout the whole structure.

3.5.3.3 *Crack observations* As noted above, cracks in concrete are at right angles to the principal tensile stress, so the orientation of cracks gives a good indication of the stress state in the wall. Since it is usually only the outside surface that can be observed, care must be taken to determine whether the cracks are caused by through-thickness tension (very serious) or external surface tension caused by bending. Diagonal cracks may, for example, indicate a flow channel of widening dimensions inside the silo.

3.5.3.4 *Ductility and delamination* Concrete is a brittle material, but most structural design relies on the assumption that the structure behaves in a ductile manner. Concrete structures achieve this by appropriate reinforcement, but where forces are applied to the structure that were not planned for in the design, brittle failures can occur. In particular, shear failures in concrete walls can cause serious cracking. Another brittle problem is that of delamination, where splitting occurs along the plane of the reinforcement. This generally occurs when the concrete is under high compressive stresses.

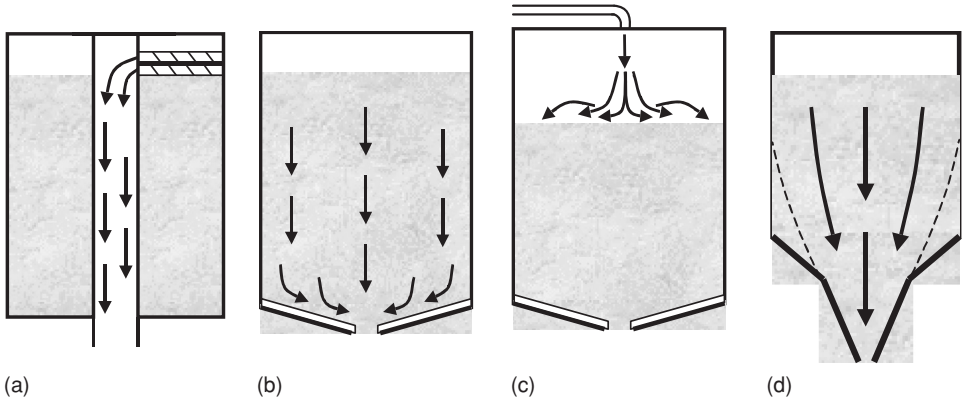


**Figure 3.26** (a) Mechanical discharge with concentric pressures; (b) air injection and air slides promote mass flow; (c) pneumatic filling of powders causes almost flat top surface; (d) expanded flow hopper gives mass flow only in the bottom hopper.

3.5.3.5 *Durability considerations* Reinforcement in concrete structures must be protected from corrosion, and the conventional manner of doing this is to have a suitable thickness of concrete 'cover' over the steel. Where large cracks are able to develop in the concrete wall, the protective effect of this cover can be lost, and a significant loss of the area of reinforcement may occur. This leads to a dramatic loss of strength and has caused failures (Elghazouli & Rotter 1996).

## 3.6 Design situations

There are many different special circumstances that can occur in silos that need special attention. Several are specifically identified in EN 1991-4 (2007), but even these require an extensive description for a full explanation. However, a few are briefly noted here so that the reader can seek further information where it is needed.

The aspect ratio of the silo is a key determinant of conditions, as noted in Figure 3.3. Where silos have an internal system of discharging (Figure 3.26a), only filling pressures need to be considered, so simpler safe designs are possible. Where air slides are used in silos containing powders that can be fluidised (Figure 3.26b), the flow pattern will be mass flow irrespective of the indications of Figure 3.21: mass flow pressure conditions must be assumed. Where powders are filled in a condition such that they are fluidised on deposition, it should be assumed that the top surface will be flat (Figure 3.26c): this matters where the silo is relatively squat. Where an expanded flow hopper is used (Figure 3.26d), the bottom part of the hopper is subject to mass flow hopper pressures, but the upper part of the hopper may be shallow and the base of the cylinder experiences mixed flow, so proper account should be taken of this.

Internal structures within silos (tubes to assist flow, flow promotion devices such as Chinese hats and cone-within-cone structures, etc.) may be subject to large forces from stored solids. Some advice on these may be found in the Australian Standard (AS 3774 1996).

Finally, where silos may be subjected to seismic loads, much care is needed. In elevated silos, a huge mass is supported on a relatively soft spring, leading to a low natural frequency which is easily excited by seismic waves. In on-ground silos, vertical compressions and high shear forces develop in the walls due to the horizontal excitation (Rotter & Hull 1989), and care must be taken to ensure that the structure is strong enough, but also to ensure adequate connection in the base details. Some information may be found in EN 1998-4 (2006).

## 3.7 Concluding remarks

This chapter has given a brief outline of the key aspects of silo pressure phenomena and their implications for potential damage to silo structures. It is evident that the subject is large and requires much more detailed treatment on many issues than is possible here. However, many references to other useful sources have been given.

Our understanding of silo pressures and their consequences for storage structures is continually expanding, sometimes as a result of new catastrophes. As a result, current advice and standards are likely to be steadily improved, and better treatments should be available for many of the questions that were imperfectly answered here. The reader is invited to seek specialist advice when new problems are encountered.

## Acknowledgements

The author wrote this chapter whilst in Hong Kong as a Royal Society Kan Tong Po Visiting Professor. The author is most grateful to the Royal Society, the Kan Tong Po fund and the Hong Kong Polytechnic University for their generous support. The chapter has drawn on understandings gained in extensive discussions with Dr Jørgen Nielsen and Prof J.G. Teng, and their contributions are gratefully acknowledged.

## References

Arnold, P.C. (May 1991) On the influence of segregation on the flow patterns in silos. *Bulk Solids Handling*, **11**(2), 447–449.

Arnold, P.C. & McLean, A.G. (November 1976) Prediction of cylinder flow pressures in mass-flow bins using minimum strain energy. *J. Eng. Ind., Trans ASME, Ser. B*, **98**(4), 1370–1374.

Arnold, P.C., McLean, A.G. & Roberts, A.W. (1980) *Bulk Solids: Storage, Flow and Handling, Tunra Bulk Solids Handling Research Associates*, 2nd edn. University of Newcastle, NSW, Australia.

AS3774 (October 1996) *Loads on Bulk Solids Containers, Australian Standard*. Standards Association of Australia, Sydney.

Chen, J.F., Rotter, J.M., Ooi, J.Y. & Zhong, Z.J. (June 2005) Flow pattern measurement in a full scale silo containing iron ore. *Chem. Eng. Sci.*, **60**(11), 3029–3041.

Dabrowski, A. (1957) *Parcie Materialow Sypkich w Leju* (Pressures from Bulk Solids in Hoppers). Archiwum Inzynierii Ladowej, Warsawa, pp. 325–328.

DIN 1055-6 (1964, 1987, 2006) *Design Loads for Buildings: Loads in Silo Containers*. DIN 1055, Part 6, Deutsches Institut für Normung, Berlin.

Drescher, A. (1991) *Analytical Methods in Bin-Load Analysis*. Elsevier, New York.

Elghazouli, A.Y. & Rotter, J.M. (February 1996) Long-term performance and assessment of circular reinforced concrete silos. *Construction Build. Mater.*, **10**(2), 117–122.

EN 1991-4 (2007) *Eurocode 1: Basis of Design and Actions on Structures, Part 4 – Silos and Tanks*. CEN, Brussels.
EN 1993-1-6 (2007) *Eurocode 3: Design of Steel Structures, Part 1.6: General Rules – Strength and Stability of Shell Structures*. CEN, Brussels.
EN 1993-4-1 (2007) *Eurocode 3: Design of Steel Structures, Part 4.1: Silos*. CEN, Brussels.
EN 1998-4 (2006) *Eurocode 8: Design Provisions for Earthquake Resistance of Structures – Part 4: Silos, Tanks and Pipelines*. CEN, Brussels.
Gaylord, E.H. & Gaylord, C.N. (1984) *Design of Steel Bins*. Prentice Hall, New Jersey.
Jaky, J. (1948) Pressures in silos. *Proceedings of the 2nd International Conference on Soil Mechanics and Foundation Engineering*, Rotterdam, Vol. 1, pp. 103–107.
Janssen, H.A. (1895) Versuche uber Getreidedruck in Silozellen. *Z. des Vereines Dtsch Ingenieure*, **39**(35), 1045–1049.
Jenike, A.W. (1961) *Gravity Flow of Bulk Solids*. Bulletin of the University of Utah, Vol. 52, No. 29, Bulletin No. 108 of the Utah Engineering Experiment Station, Salt Lake City, Utah.
Jenike, A.W. (1964) *Storage and Flow of Solids*. Bulletin of the University of Utah, Vol. 53, No. 26, Bulletin No. 123 of the Utah Engineering Experiment Station, Salt Lake City, Utah (revised November 1976).
Jenike, A.W. (February 1967) Denting of circular bins with eccentric drawpoints. *J. Struct. Div., ASCE*, **93**(ST1), 27–35.
Jenike, A.W., Johanson, J.R. & Carson, J.W. (February 1973) Bin loads – Parts 2, 3 and 4: concepts, mass flow bins, funnel flow bins. *J. Eng. Ind., Trans. ASME*, **95**(1, Series B), 1–5, 6–12, 13–16.
Ketchum, M.S. (1907) *Design of Walls, Bins and Grain Elevators*, 1st edn. McGraw-Hill, New York (2nd edn, 1911; 3rd edn, 1919).
Koenen, M. (1895) Berechnung des Seitenund Bodendrucks in Silos. *Zentralbl. Bauverwaltung*, **16**, 446–449.
Muir Wood, D. (1990) *Soil Behaviour and Critical State Soil Mechanics*. Cambridge University Press, Cambridge, England.
Nanninga, N. (November 1956) Gibt die ubliche Berechnungsart der Drucke auf die Wande und den Boden von Silobauten Sichere Ergebnisse. *Die Ingenieur*, **68**(44).
Nielsen, J. (1998) Pressures from flowing granular solids in silos. *Phil. Trans. R. Soc., Lond. A*, **356**(1747), 2667–2684.
Ooi, J.Y., Rotter, J.M. & Pham, L. (1990) Systematic and random features of measured pressures on full-scale silo walls. *Eng. Struct.*, **12**(2), 74–87.
Pieper, K. & Stamou, K. (March 1981) Lasten in Niedrigen Silos. Lehrstuhl für Hochbaustatik, Technische Universität Braunsweig, 94 pp.
Pieper, K. & Wenzel, F. (1964) *Druckverhältnisse in Silozellen*. Wilhelm Ernst und Sohn, Berlin.
Rankine, W.J.M. (1857) On the stability of loose earth. *Phil. Trans. R. Soc., Lond.*, **147**, 9.
Rotter, J.M. (1986a) On the significance of switch pressures at the transition in elevated steel bins. *Proceedings of the Second International Conference on Bulk Materials Storage Handling and Transportation, Institution of Engineers*, Wollongong, Australia, pp. 82–88.
Rotter, J.M. (1986b) The analysis of steel bins subject to eccentric discharge. *Proceedings of the Second International Conference on Bulk Materials Storage Handling and Transportation*, Institution of Engineers, Wollongong, Australia, pp. 264–271.
Rotter, J.M. (1999) Flow and pressures in silo structural integrity assessments. *Proceedings of the International Symposium: Reliable Flow of Particulate Solids III*, Porsgrunn, Norway, August 1999, pp. 281–292.
Rotter, J.M. (2001a) *Guide for the Economic Design of Circular Metal Silos*. Spon, London.
Rotter, J.M. (2001b) *Pressures, Stresses and Buckling in Metal Silos containing Eccentrically Discharging Solids*. Festschrift Richard Greiner, TU Graz, Austria, pp. 85–104.
Rotter, J.M. (2001c) *Report on Damage to the Raw Meal Silo at Cebu*. Technical Investigation Report C01-05, School of Civil and Environmental Engineering, University of Edinburgh.
Rotter, J.M. & Hull, T.S. (1989) Wall loads in squat steel silos during earthquakes. *Eng. Struct.*, **11**(3), 139–147.
Rotter, J.M., Ooi, J.Y. & Zhong, Z. (2006) Critical pressure conditions in silos. *Proceedings of the 5th International Conference for Conveying and Handling of Particulate Solids*, Sorrento, Italy, 27–31 August, 6 pp.
Rotter, J.M., Pham, L. & Nielsen, J. (1986) On the specification of loads for the structural design of bins and silos. *Proceedings of the Second International Conference on Bulk Materials Storage Handling and Transportation*, Institution of Engineers, Australia, Wollongong, July 1986, pp. 241–247.
Schmidt, K.H. & Stiglat, K. (1987) Anmerkungen zur Bemessungslast von Silos. *Beton und Stahlbetonbau*, **9**, 239–242.
Teng, J.G. & Rotter, J.M. (1991) The strength of welded steel silo hoppers under filling and flow pressures. *J. Struct. Eng., ASCE*, **117**(9), 2567–2583.

Walker, D.M. (1964) *A Theory of Gravity Flow of Cohesive Powders*. Central Electricity Generating Board, UK, SW Region, R&D Dept, Report No 22.

Walker, D.M. (1966) An approximate theory for pressure and arching in hoppers. *Chem. Eng. Sci.*, **21**, 975–997.

Walters, J.K. (1973) A theoretical analysis of stresses in silos with vertical walls. *Chem. Eng. Sci.*, **28**, 13–21.

Wood, J.G.M. (1983) The analysis of silo structures subject to eccentric discharge. *Proceedings of the Second International Conference on Design of Silos for Strength and Flow*, Stratford-upon-Avon, pp. 132–144.